PIONEER Data Acquisition Development Update

Jack Carlton
University of Kentucky

Outline

You can find this presentation in my notes

Links:
https://github.com/jaca230/joplin_notes_page
or
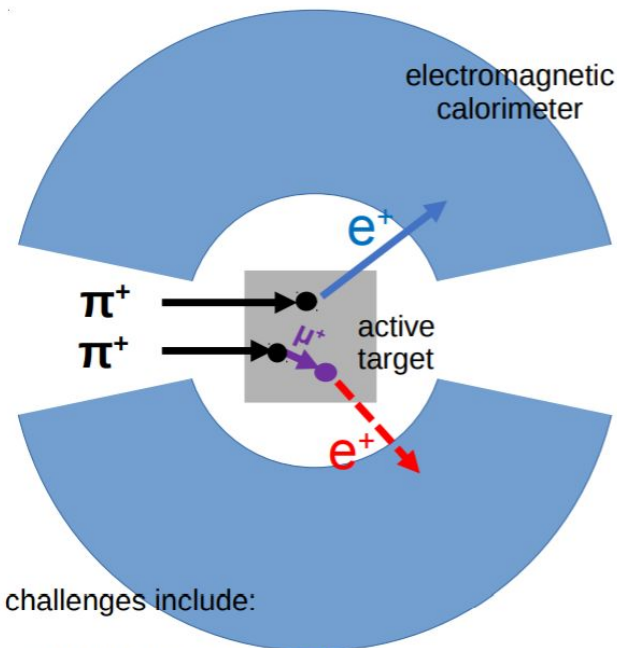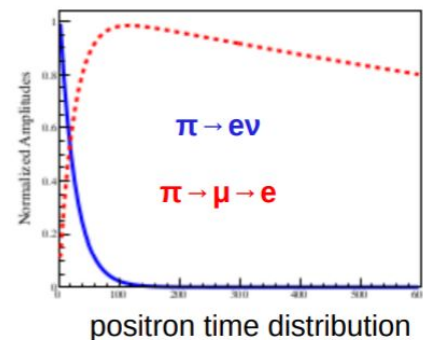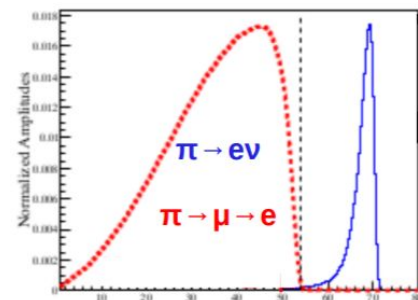https://tinyurl.com/jack-uky-notes

PIONEER Refresher

PIONEER Experimental Proposal

- **LXe (or LYSO) has shorter decay time**
  - ~ 25 ns

- **Allows experiment to run at much higher rate**
  - ~300kHz (phase 1)
  - ~2000kHz (phase 2 and 3)

- **"active target", muons and pions are "tracked"**

electromagnetic calorimeter

e^+

π^+

π^+

μ^+

active target

e^+

challenges include:
- calorimeter energy tail
- in-flight pion decay
- beam, positron pileup

$\pi \to e\nu$

$\pi \to \mu \to e$

positron energy distribution

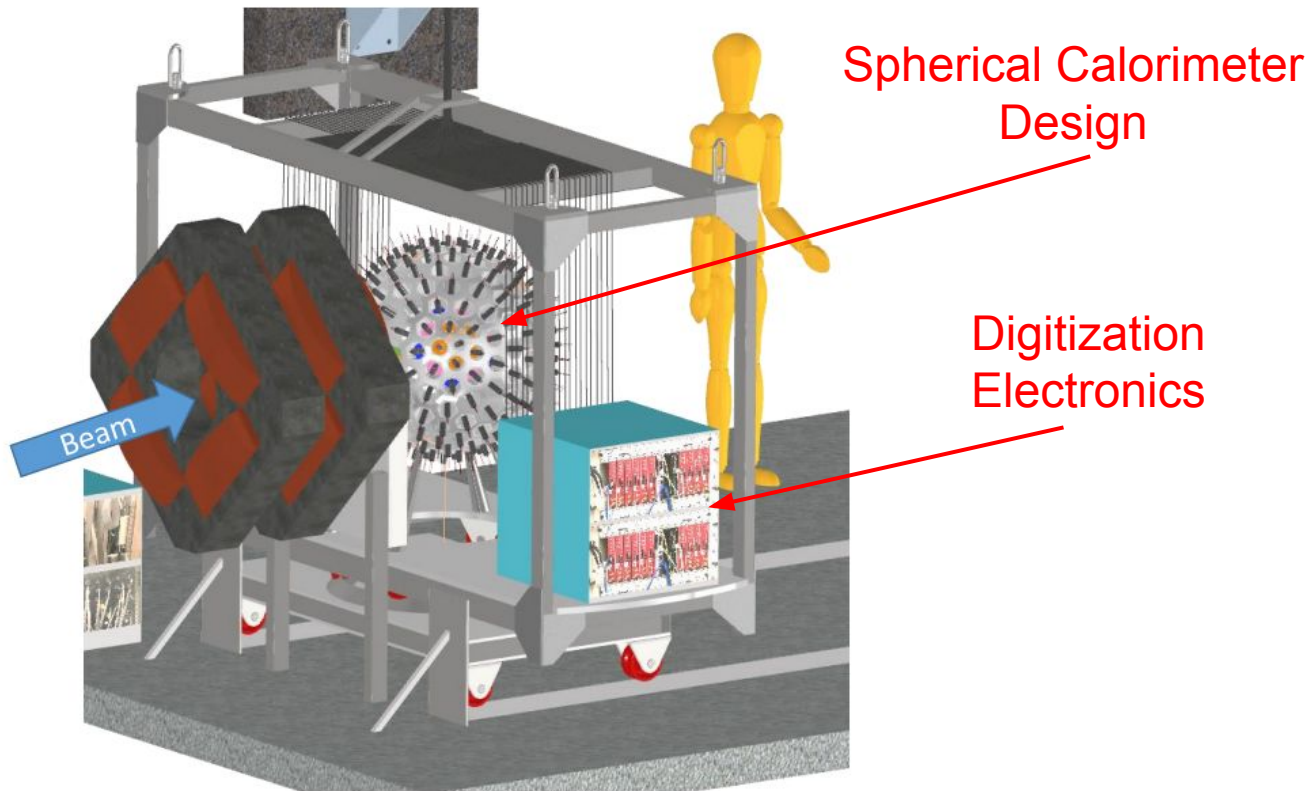$\pi \to e\nu$

$\pi \to \mu \to e$

positron time distribution

3D Render Experiment

Not Pictured:

- ATAR (inside Calo)
- Tracker (a shell around ATAR, inside Calo)
- VETOs, T0, etc.
- DAQ Computers

Spherical Calorimeter Design

Digitization Electronics

Beam

How PIONEER Will Improve the $R_{e/\mu}$ Measurement

- 5D space-time-energy active pion stopping target (ATAR)
  - Reduce e^+ energy tail, identify beam pileup, identify $\pi \rightarrow \mu\nu_\mu$ decays

- Large acceptance, deep radiation length calorimeter
  - LXE or LYSO for high resolution, fast response, small tail

- Fast electronics, high-speed acquisition
  - Giga sample/second digitizers, new gen PCIe readout

- PSI high intensity pion beams
  - 2 mA proton beam, large acceptance beamline

Midas Framework

- C/C++ (mostly)
  package of modules for
  - run control,
  - expt. configuration
  - data readout
  - event building
  - data storage
  - slow control
  - alarm systems
  - Etc.
- Can link with custom
  software

Example g-2 Midas Webpage

Test Stand DAQ Development

Overview

- The test stand DAQ is used throughout the PIONEER collaboration
  - Helps test and develop crucial experiment components

- Built on top of g-2 DAQ hardware and software

Hardware Side

Software Side
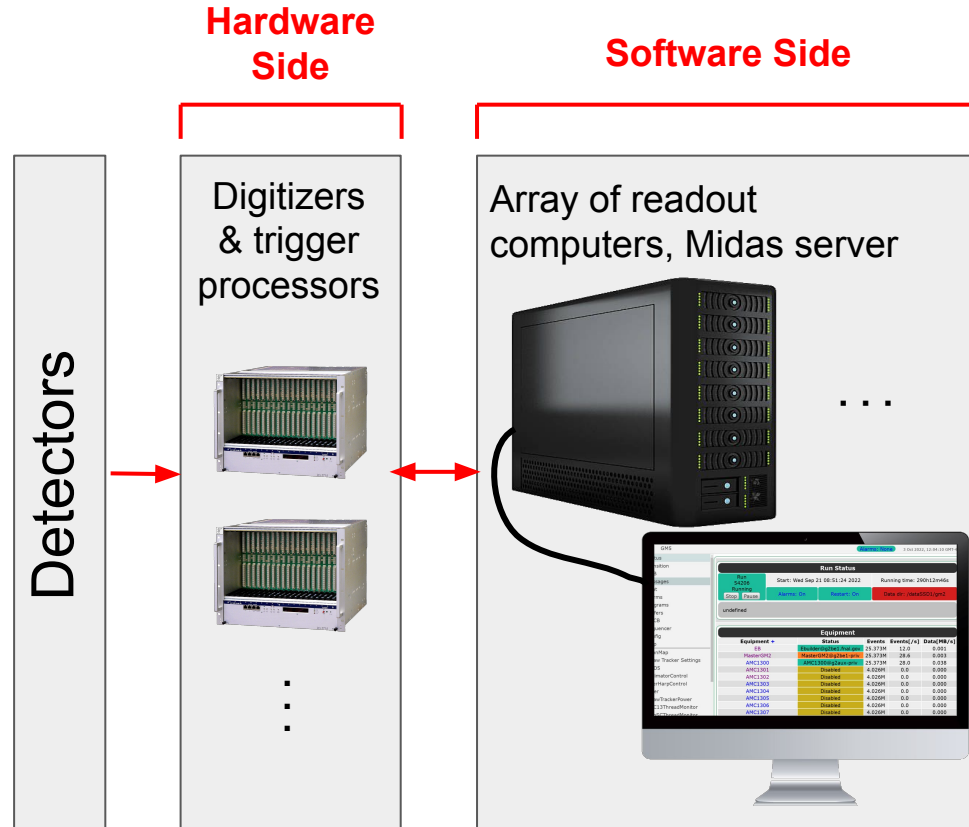
Hardware - Labeled Crate
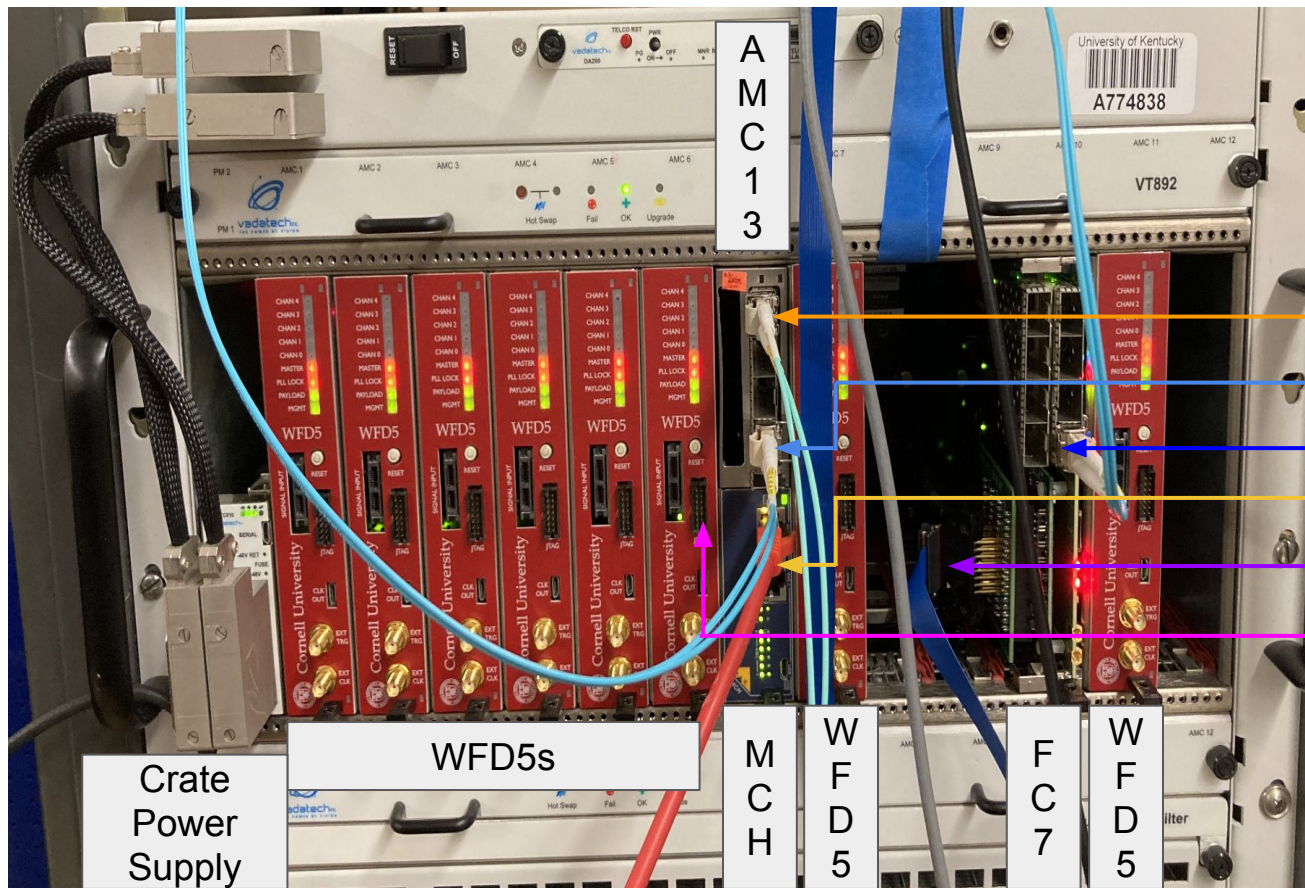
Note: AMC13 and MCH are half slot modules

10GbE out (data) AMC13→desktop

Trigger in AMC13

Trigger out FC7

1GbE MCH in/out (comm.)

FC7 Trigger in

WFD5 5-channel, differential signal in (no connection in this picture)

Software - Adjustment Made

- ● Generalized the frontend code
  - ○ Crate contents no longer assumed
  - ○ Added option to remove unneeded hardware reliance (meinberg card)
  - ○ Added support for arbitrary number of crates
  - ○ Added scripts for ease of setup and use

- ● Added features
  - ○ Timing monitoring
  - ○ Data quality Monitoring (DQM)
  - ○ System resource monitoring
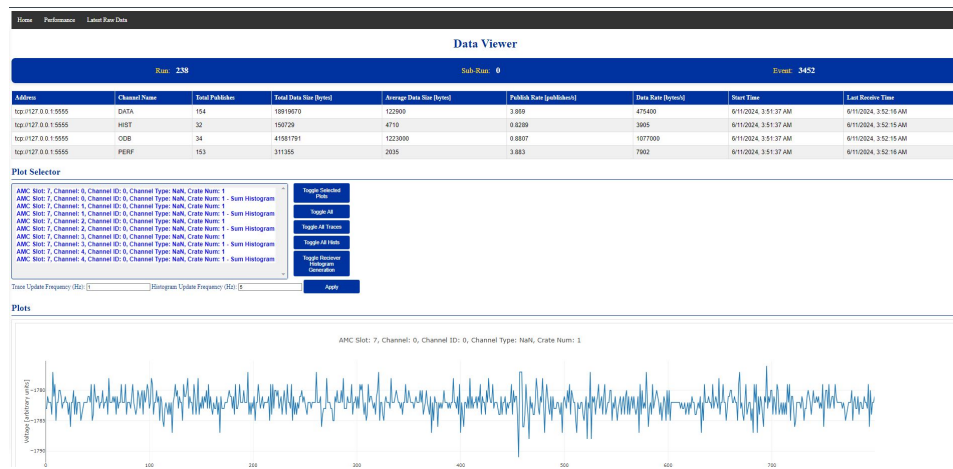
Generalized Teststand DAQ DQM Webpage

Documentation

- Setup of the teststand DAQ is not straightforward
  - Custom software and hardware
  - Specific software and hardware configurations
- Created documentation to aid users
  - Website version on github pages
    https://jaca230.github.io/teststand_daq_manual/
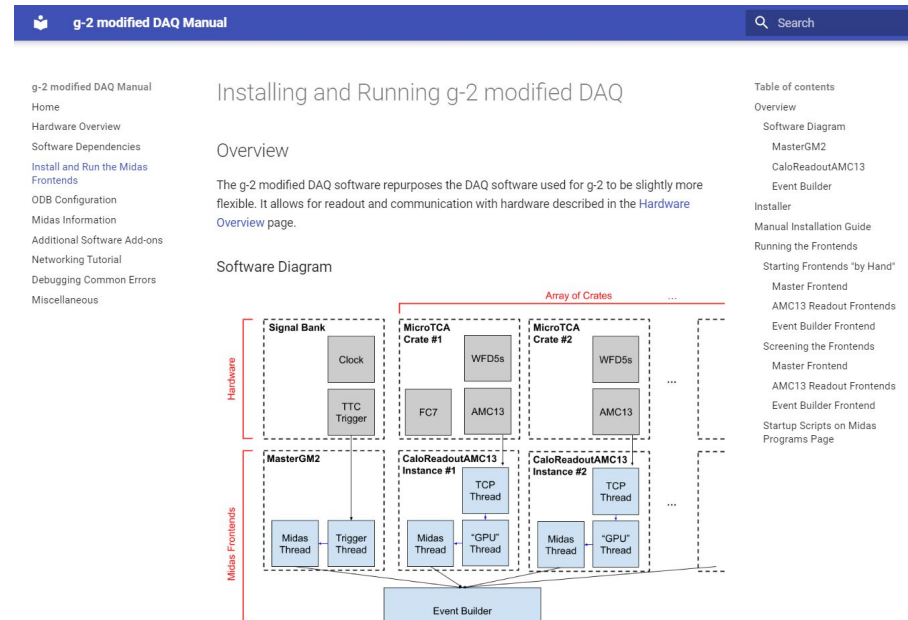
A page from the manual webpage

Use Cases

- LYSO tests at CENPA

- 2023 PSI Test Beam

- Liquid Xenon tests at TRIUMF

- Experiments at PSI
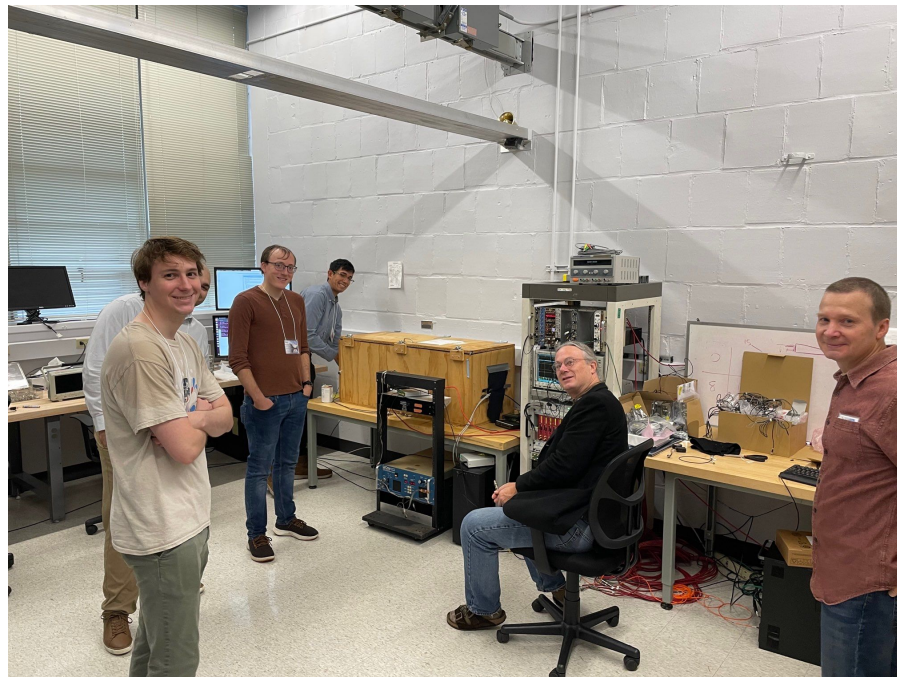
Setting up test stand at University of a Washington (on a rainy day)

2023 PSI Test Beam

Overview

- PIONEER LYSO Calorimeter test
    - November 15 - 29, 2023

- Made measurements using LYSO
  scintillator crystals to determine if
  they are an adequate candidate for
  PIONEER's calorimeter
    - **Energy resolution**
    - Timing resolution
    - Spatial resolution

Contributions

- Repurposing g-2 DAQ Software

- Flexible Pipeline for Data Quality Monitor

- Beamtime "Live" DAQ Maintenance

- Onsite preliminary data analysis
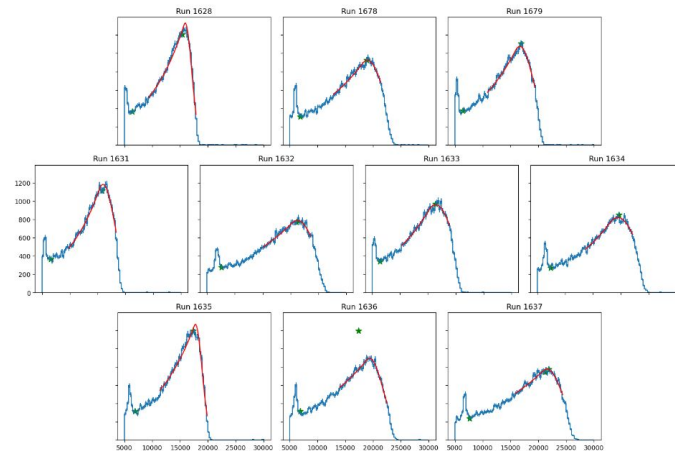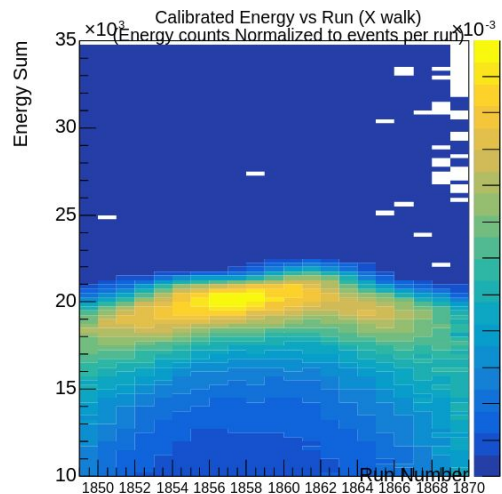
Examples of preliminary analysis work done at PSI

Experiment Diagram - Conceptual Picture

Citation: Testing Lepton Flavor Universality and CKM Unitarity with Rare Pion Decays in the PIONEER experiment, PIONEER collab (pg. 20, arxiv: 2203.05505)

j.carlton@uky.edu
III. 2023 PSI Test Beam (Slide 18/37)
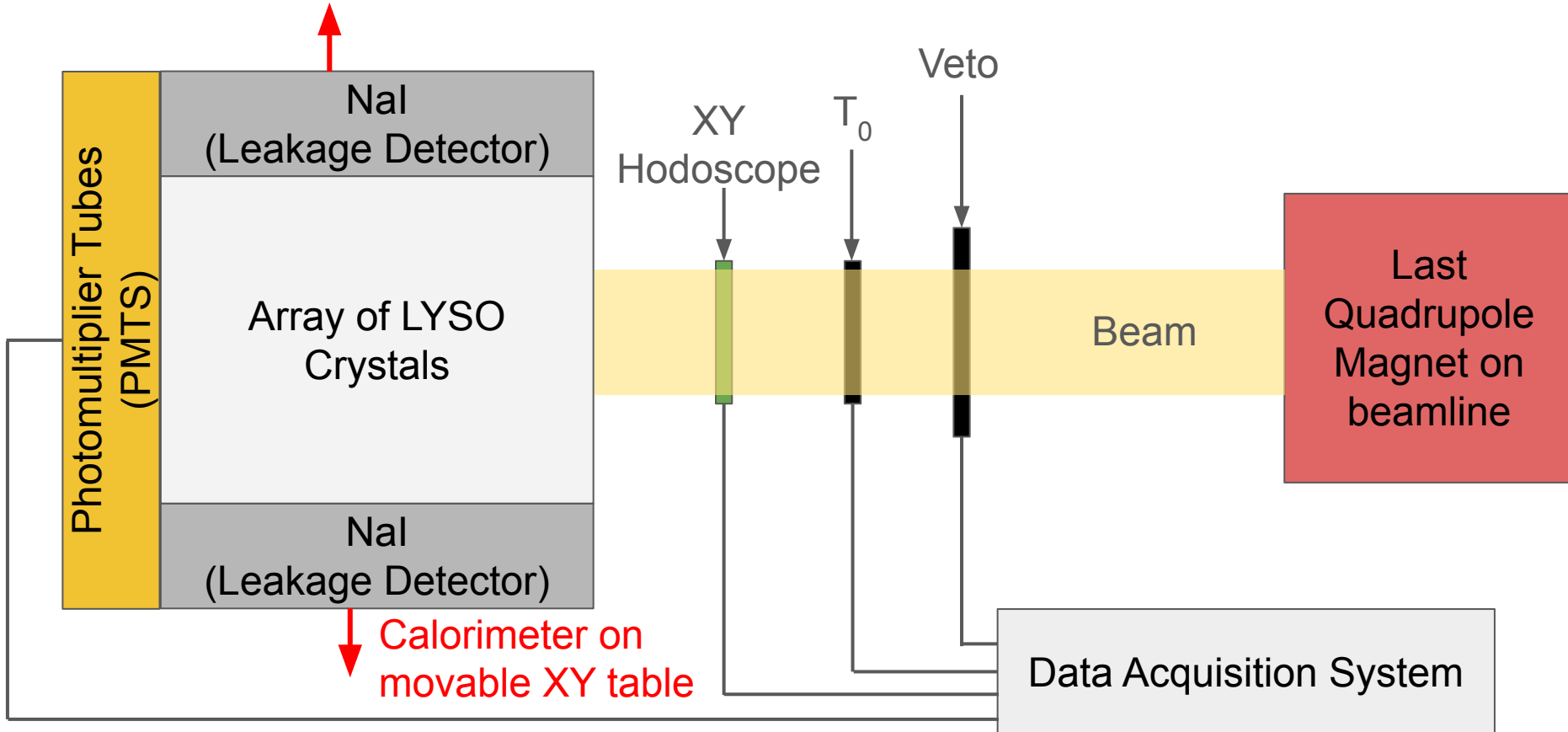
Experiment Diagram - Labeled Picture
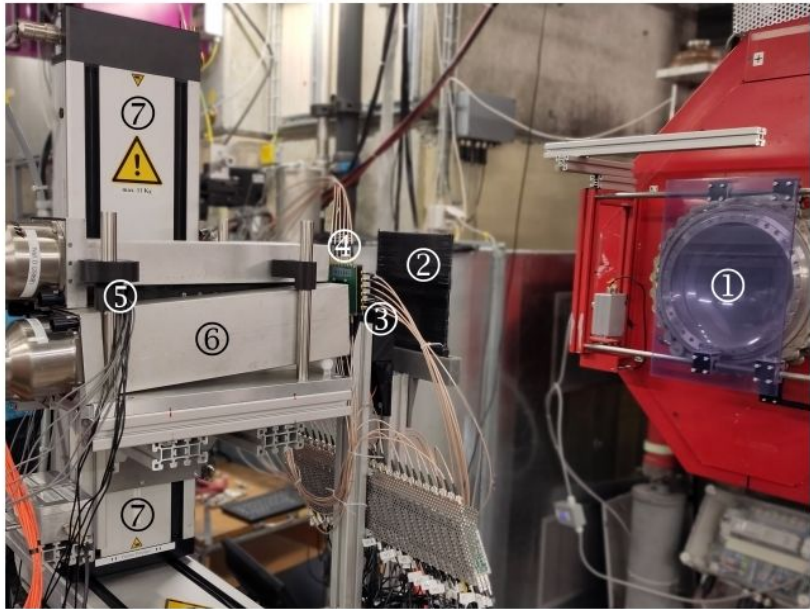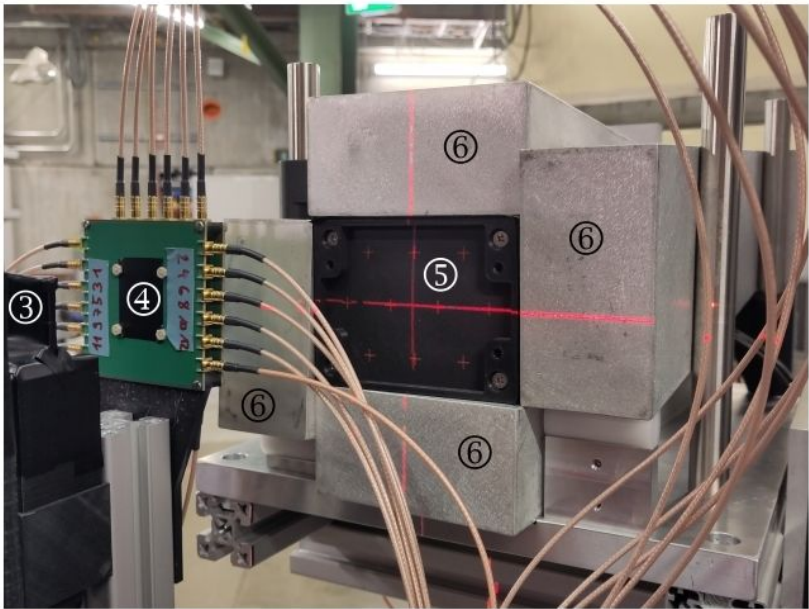
(a)　　　　　　　　　　　　　　　(b)

A full view of the detector setup during the PSI test beam (a) and a close-up of the calorimeter front-face during laser alignment (b). Positrons from the last quadrupole magnet ① pass through the VETO counter ②, T0 ③, and beam hodoscope ④ before depositing energy in the LYSO array ⑤. The LYSO crystals, along with the surrounding NaI detectors ⑥, are mounted on a movable XY table ⑦.

Hodoscope

- 2 Layers of 12 scintillator strips
  - Layers offset by 90 degrees
- 1 mm x 1 mm "pixels" created by strip intersections
  - Allows for finer positioning data
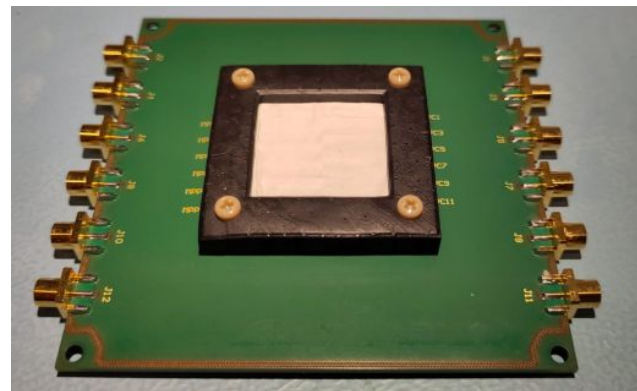
1 Hodoscope layer, 12 SiPMs connecting to 12 BC404 plastic scintillator 2mm wide bars
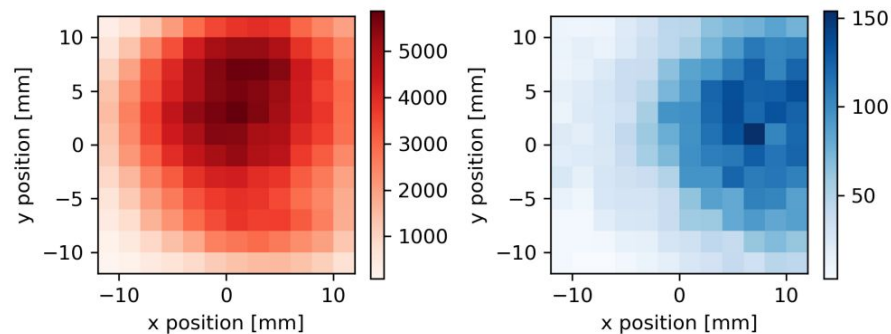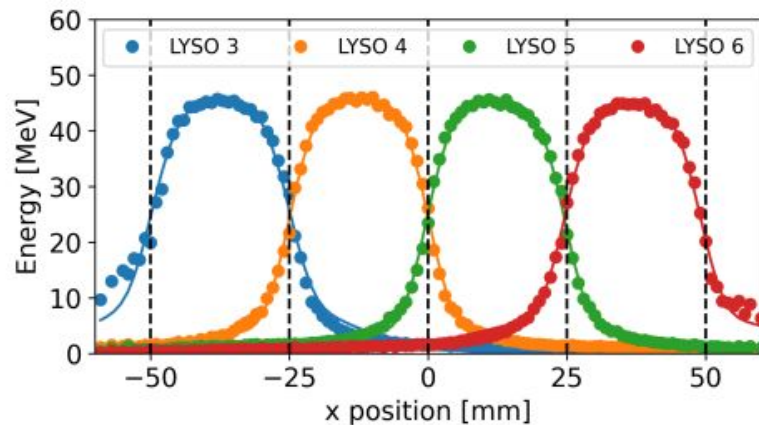
Beam Profile: Red - positrons, Blue - muons

LYSO Calorimeter

- Constructed from an array of 10 LYSO crystals
  - NaI for leakage detection
- X_0 = 1.14 cm
- R_M = 2.07 cm

Front-facing image of LYSO calorimeter
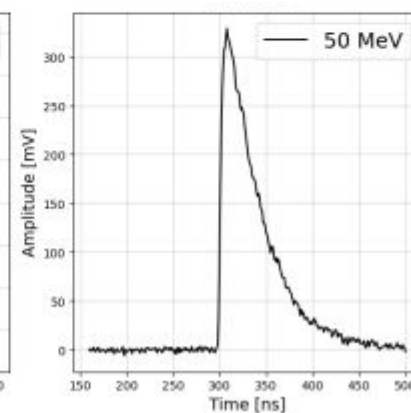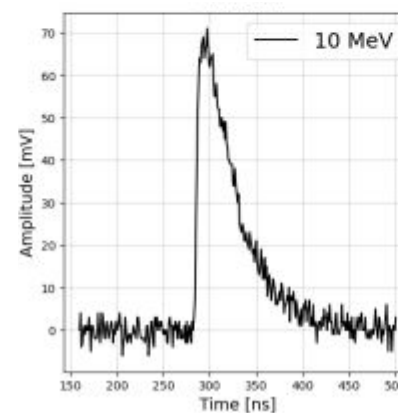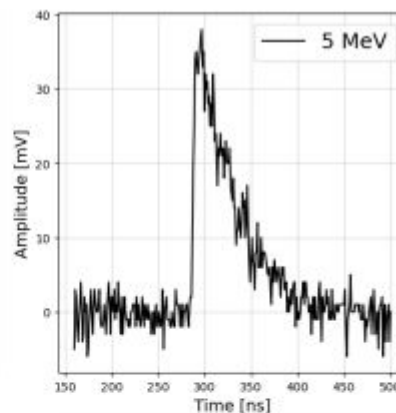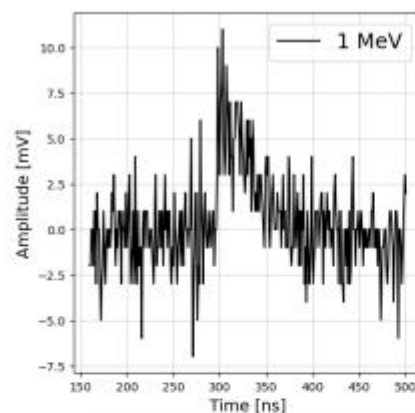
Results - Energy Resolution

- Measured an energy resolution of
  ΔE/E = 1.55 ± 0.05%
  - Published as 1.80, recently improved with better integration strategy
  - 70 MeV ≈ e energy in $\pi \rightarrow e\nu_e$

- Over two times better than reported results for previous generation LYSO crystals

- Similar to liquid xenon energy resolution
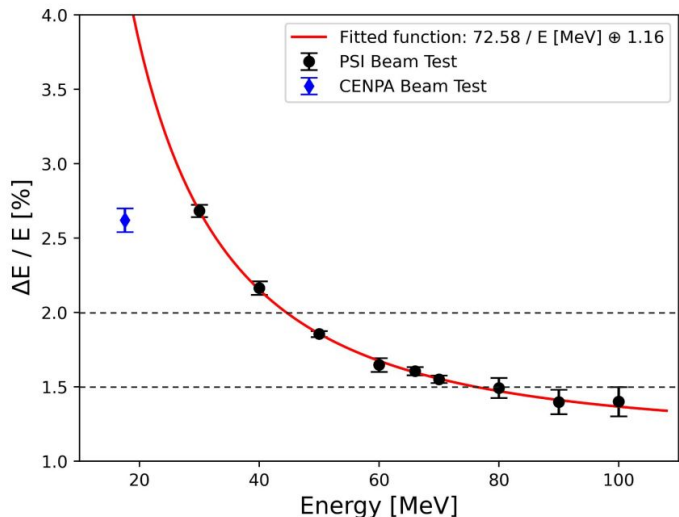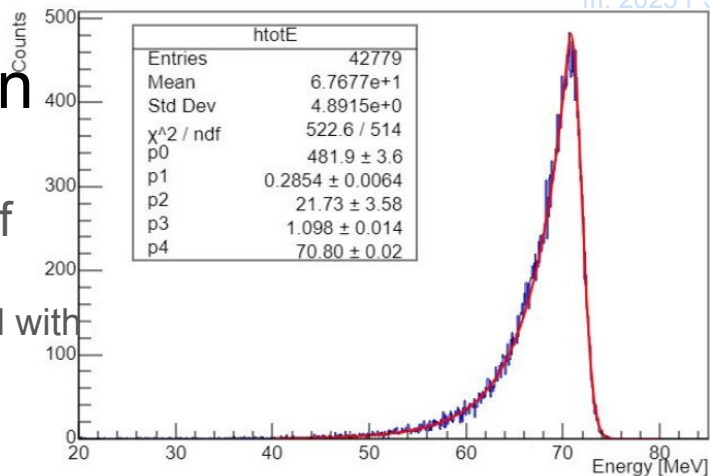
PIONEER DAQ Development

Development Overview

- DAQ work is split into a "hardware side" and "software side"
  - Cornell mostly handles the hardware side
  - UKY mostly handles the software side

- Hardware side goals:
  - Design a flexible system to handle real time data processing, digitizations, and triggers
  - Communication to software side over PCIe

- Software side goals:
  - Handle electronics readout and communication over PCIe
  - Handle data processing and compression

Citation: Testing Lepton Flavor Universality and CKM Unitarity with Rare Pion Decays in the
PIONEER experiment, PIONEER collab (pg. 20, arxiv: 2203.05505)

j.carlton@uky.edu
IV. PIONEER DAQ Development (Slide **24**/37)

Proposed Framework

arXiv:2203.05505

Citation: Testing Lepton Flavor Universality and CKM Unitarity with Rare
Pion Decays in the PIONEER experiment, PIONEER collab (pg. 21)

j.carlton@uky.edu
IV. PIONEER DAQ Development (Slide **25**/37)
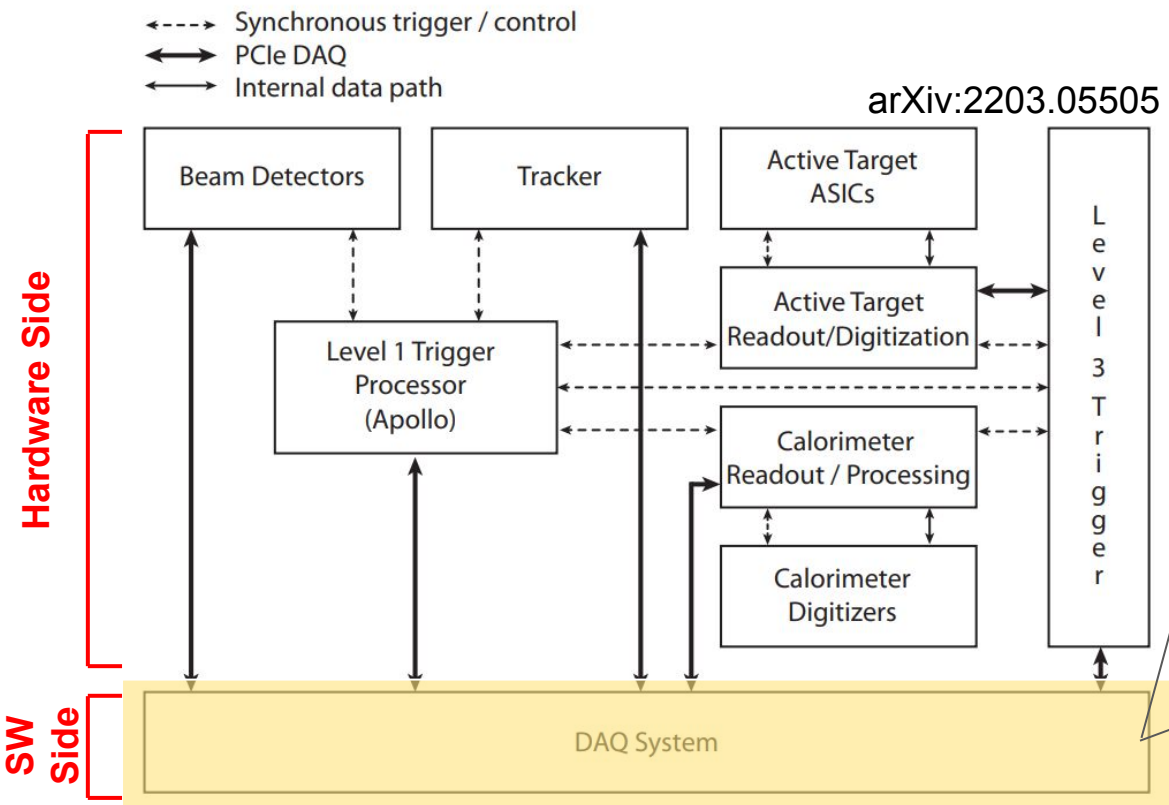
Proposed Framework

arXiv:2203.05505
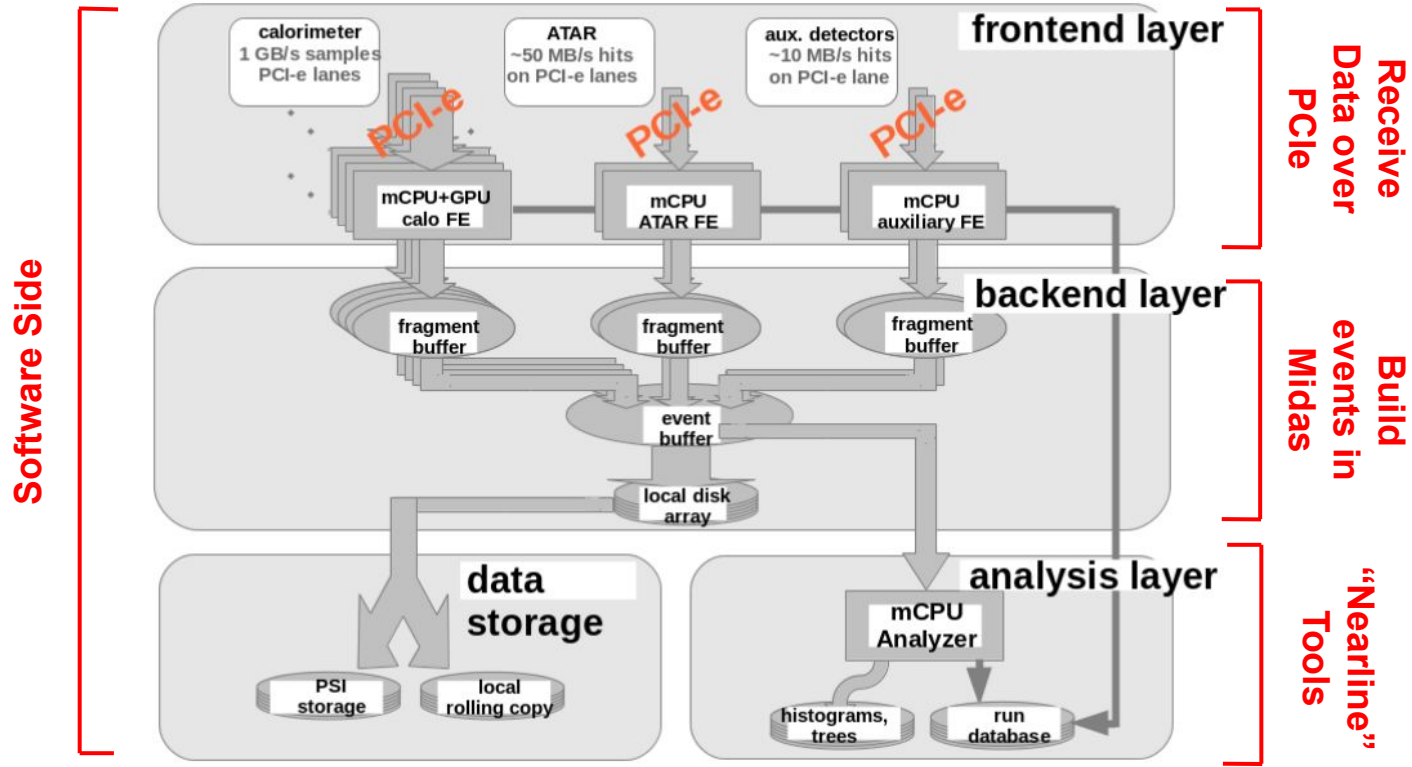
Proposed Experimental Hardware

- Using APOLLO system (no more µTCA crates)
- Data is moved using "Firefly" optical flyover system
  - 25 gb/s > 10gb/s links from g-2
- Data received by desktop through Firefly PCIe cards

Firefly PCIe board

Command Module (CU)   Service Module (BU)
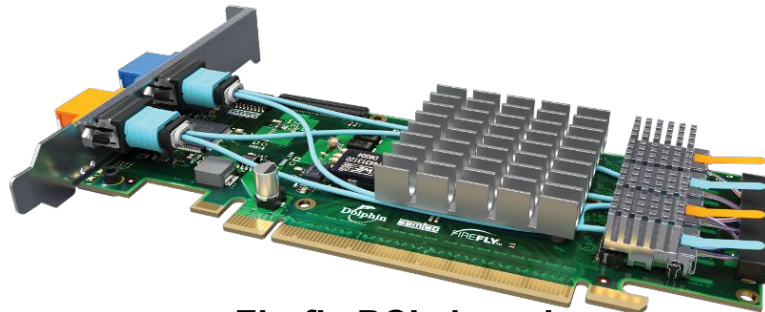
Mock Experimental Hardware - Our Development FPGA

- Using Nereid Development board
  - Kintex-7 FPGA
  - Data transfer over PCIe
  - Onboard RAM (data buffers)
  - FMC module input
- Why this board?
  - More learning resources
  - Has components to simulate real experimental hardware
- Limitations:
  - Only supports 5 GT/s (equivalent to PCIe 2)
  - Only 4 lanes (max throughput 2 GB/s)

Nereid K7 PCI Express FPGA Development Board

Mock Experimental Hardware - FPGA Firmware

- Using Xilinx intellectual property (IP) blocks in Vivado
  - IP blocks configured by development board settings

- Allows for direct memory access (DMA) transfer over PCIe between card and host
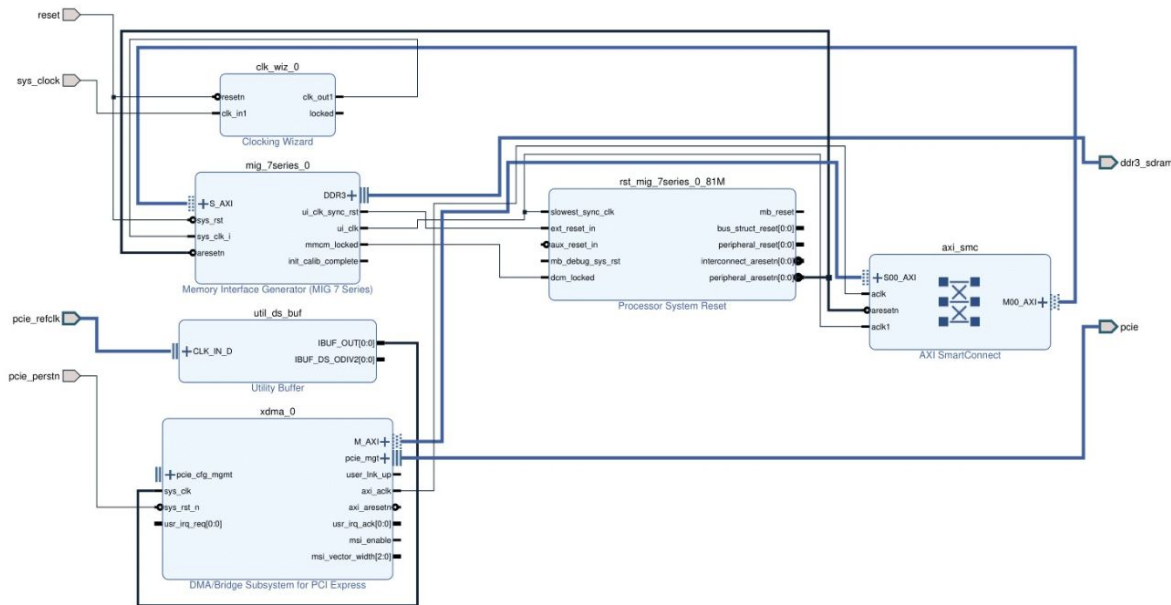
Block diagram for DMA transfer between board RAM and host (desktop) RAM

Data Rates Achieved

- More interested in read/Card-to-host (c2h) transfer rates
- Transfer rates are faster for larger data transfer sizes
- Using multiple channels, highest data throughput through midas was **1GB/s**
- This number is largely limited by the Nereid development board's hardware
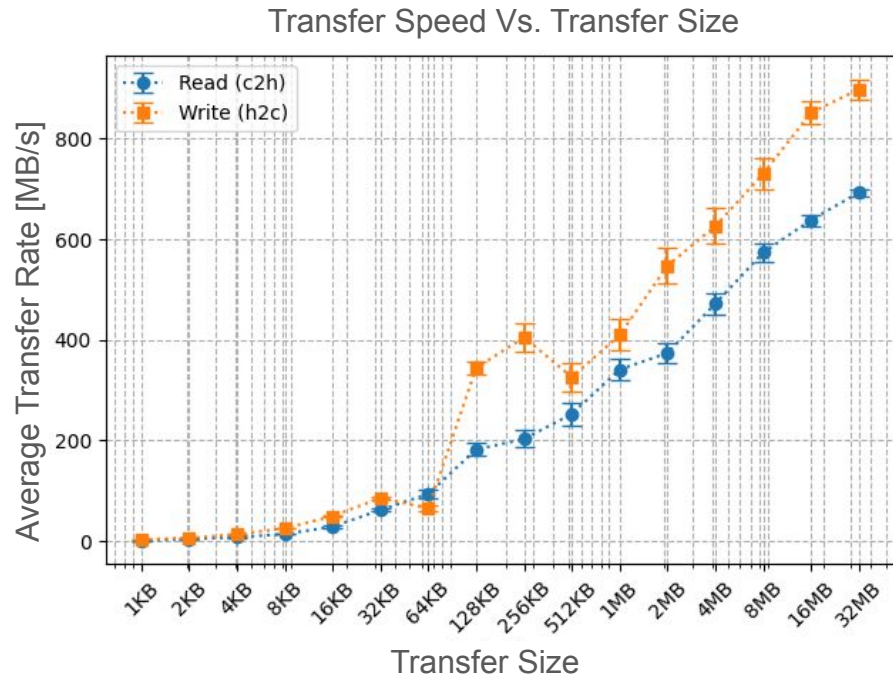
DMA transfer rate vs transfer size over one channel

Template Fitting - Example

- Can construct a continuous template for our traces $T(t)$
- Can fit traces using template:
  $$f(t) = A \cdot T(t - t_0) + B$$
- Storing unfit traces takes ~12 bits per ADC sample
- Storing residuals takes ~4 bits per ADC sample
- By fitting, we can compress the data by a **factor of ~3**

PSI Example LYSO Signal with Fit

Signal - Fit

Range = ~16
= 4 bits
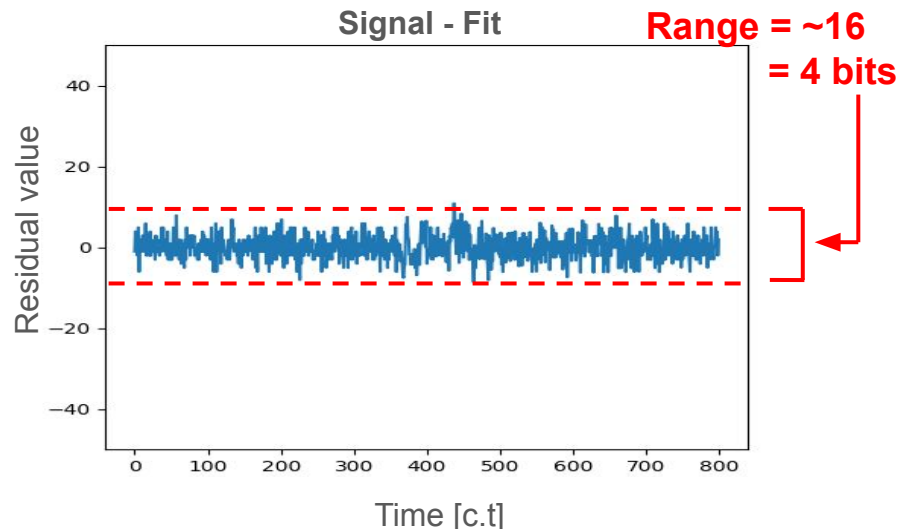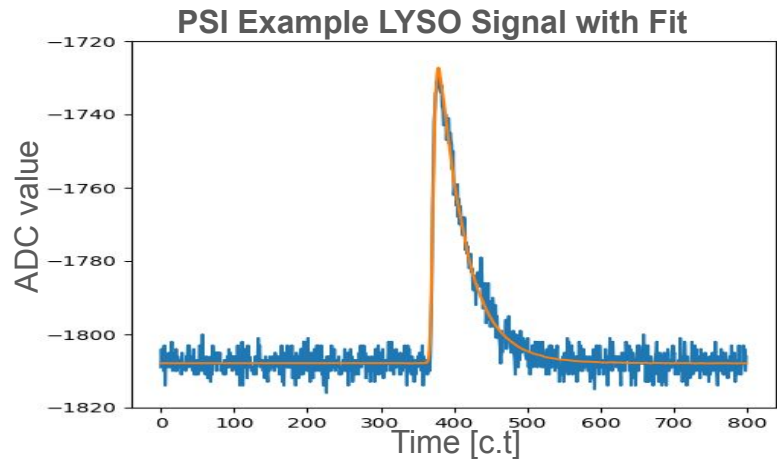
Template Fitting - Applied

- Data from PSI test beam

- Each vertical slice corresponds to pdf $p_i(x_i)$

- Template fit drastically reduces spread of data
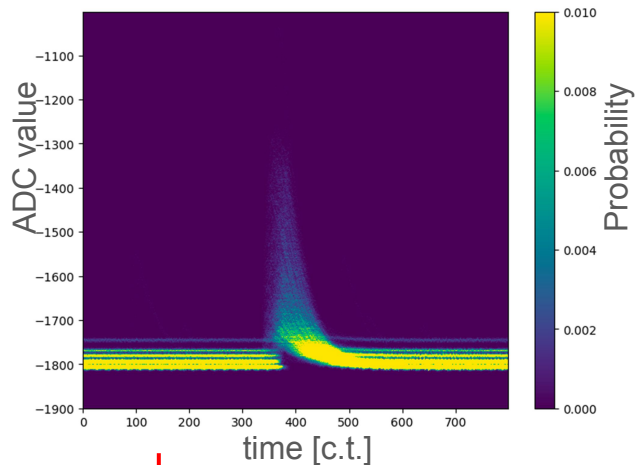
Template fitting
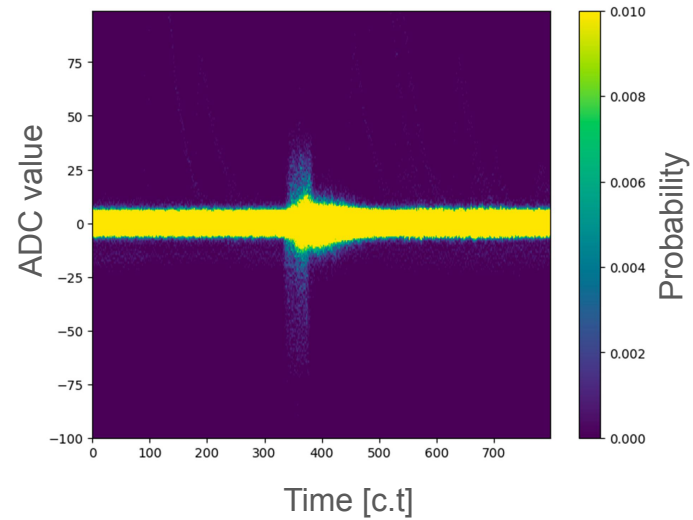
Theoretical Best Compression

- For lossless compression, the best possible compression rate is the entropy rate
- Entropy rate of pedestal part of signal is **3.4 bits per ADC sample**
  - A perfect fit would reduce signal to pedestal noise
- Best possible data storage rate 3.5 GB/s → **~1 GB/s**
  - Assumes similar noise to PSI test beam data
- Realistically the data storage rate depends how good our fit is
  - Assuming entropy rate of ~5 bits/sample 3.5 GB/s → ~1.5 GB/s

Entropy Rate Formula

$$H(X_i) = \sum_{\text{traces}} p(X_i) \log_2 \left(p(X_i) \right)$$

$$X_i \equiv \text{Random variable for } i^{\text{th}} \text{ ADC sample}$$

Entropy Rate of PSI Test Beam Data After Fitting
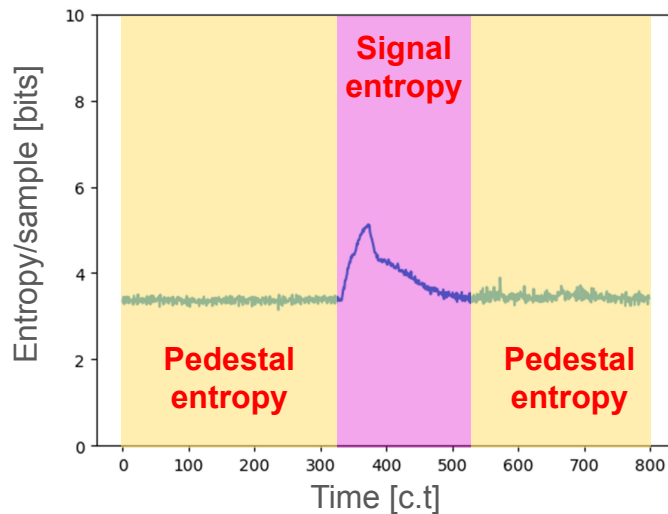
Current and Future Work

ATAR Teststand DAQ (Naludaq)

- Integrate Nalu's HDSoC digitizer output with MIDAS for synchronized, multi-detector event construction
  - Also utilize existing custom MIDAS-linked software
- Use Nalu's Python library for integration
  - Current readout via UART interface
  - Incorporate Nalu library into MIDAS frontend

Nexys A7 Video Board with Nalu's HDSoC Digitizer Attached as an FMC module
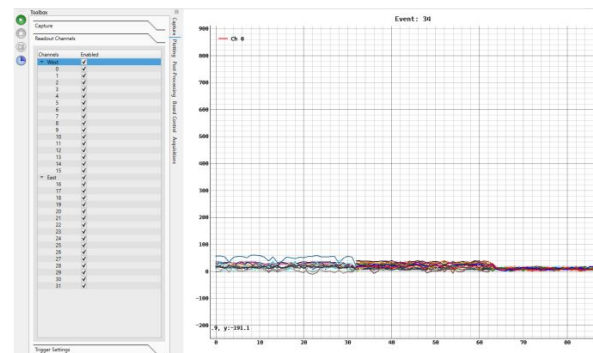
NaluScope Program Screenshot with Noise Traces

FPGA Firmware Additions

- Added MicroBlaze IP Block
- Allows the FPGA to run C++ code to edit onboard DDR3 RAM
  - Can code data generation simulators
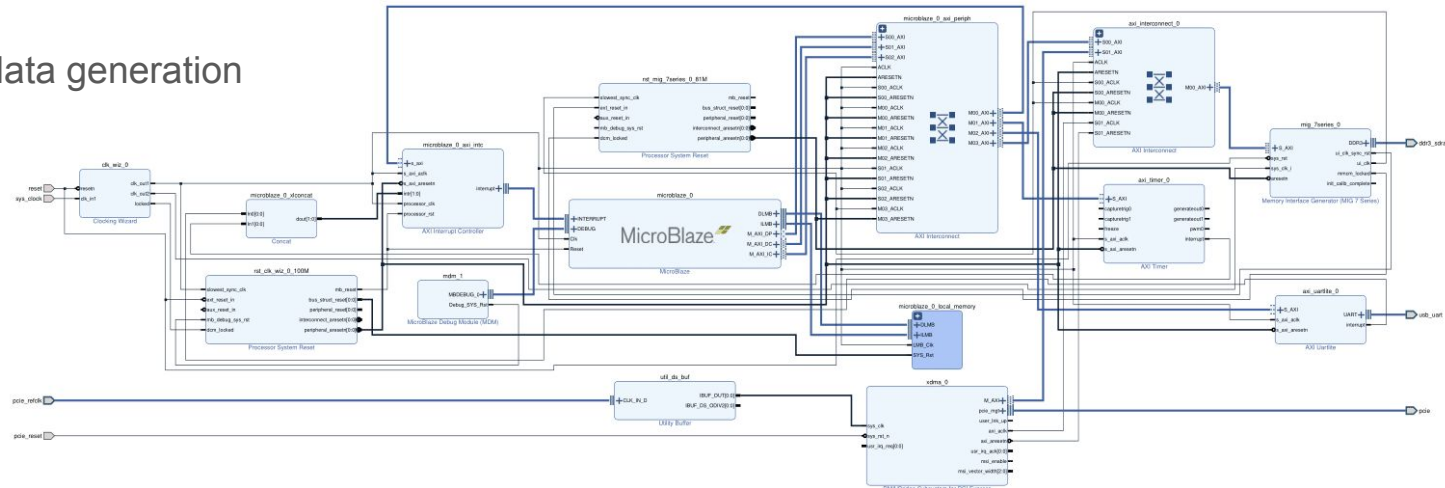
Block diagram for PCIe DMA transfer with microblaze

Generalizing and Optimizing Software

- Write modular software
  - Will make experiment DAQ code much more manageable in the future

- Optimize and adjust readout, compression, and other libraries (as needed)

- Write simple and scalable midas frontends
  - Implement libraries above
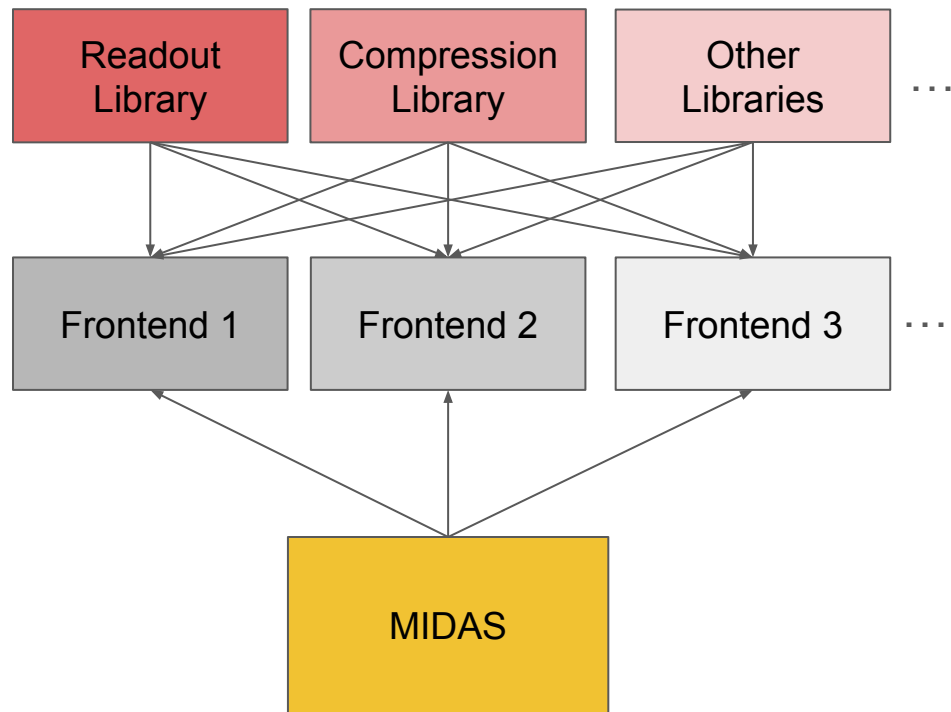
Dependency Diagram

PIONEER Demonstrator

- "Full" experiment demonstrator
- Prototypes for all detectors
  - Small number of ATAR Layers (16 layers)
  - Small spherical segment of tapered LYSO crystals (12 crystals)
  - Some spherical "shell" segment of tracker
- DAQ handles event construction
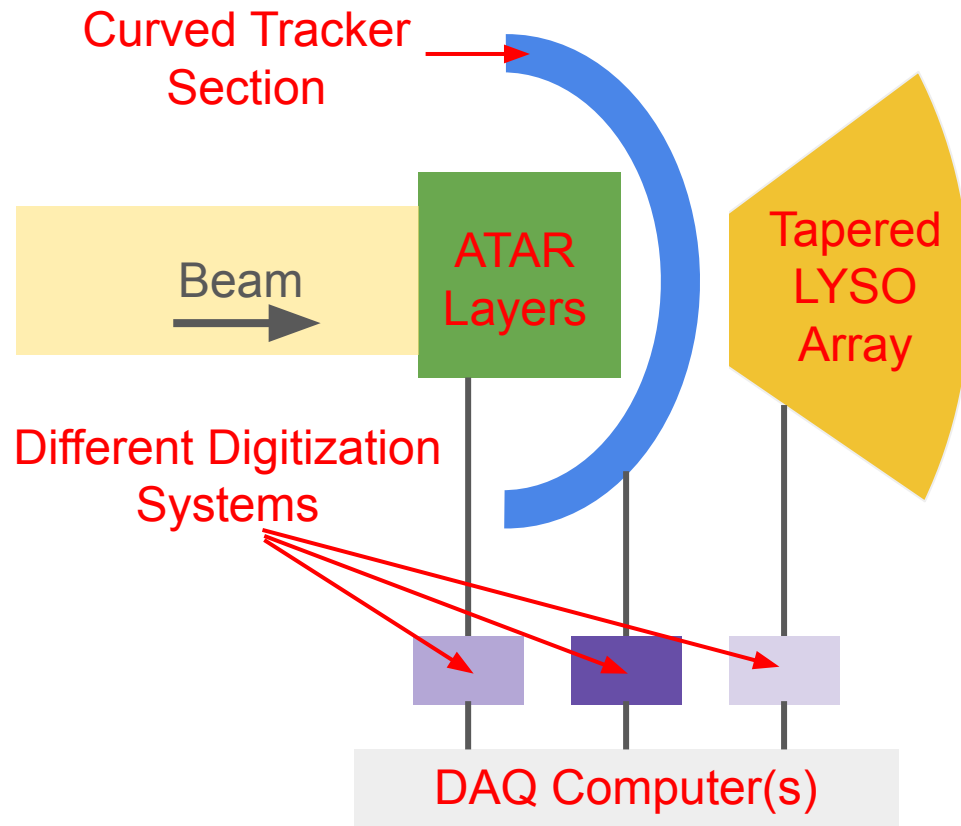
Auxiliary Slides

Background Physics

$\pi \rightarrow e\nu_e$ and $\pi \rightarrow \mu\nu_\mu$
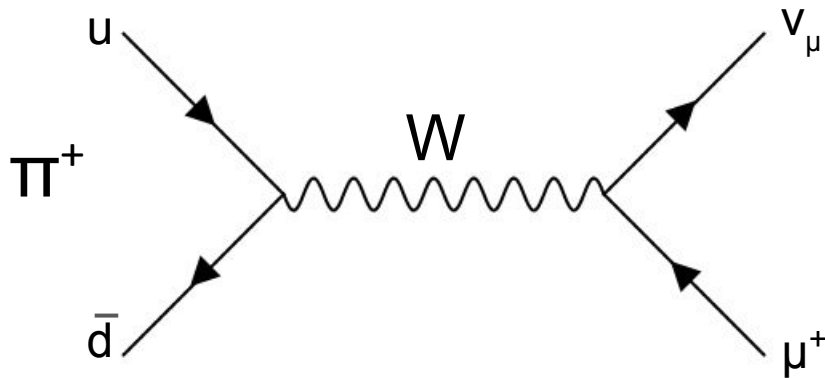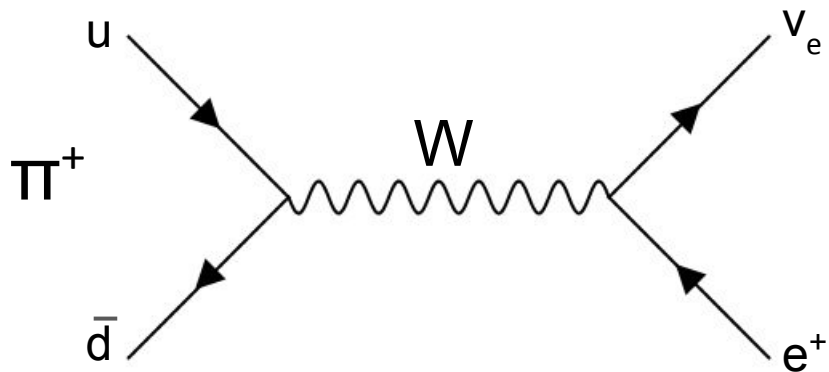
- Corresponding diagrams for π^-
- Tau decay forbidden
  - tau too massive ~ 1000 MeV/c^2
  - Pion ~ 100 MeV/c^2
- Muon decay more likely
  - branching fraction of 0.999877

Helicity Suppression (Why is Muon Decay Most Likely?)

- Naively, $\Gamma \propto p'$ → electron decay more likely
- Weak force only affects left-handed (LH) chiral particle states and right-handed (RH) chiral anti-particle states
- Neutrinos are all LH chirality
- $m_\nu \ll E$ means LH neutrino chirality → LH (negative) neutrino helicity
- Conservation of momentum → anti-lepton is LH (negative) helicity
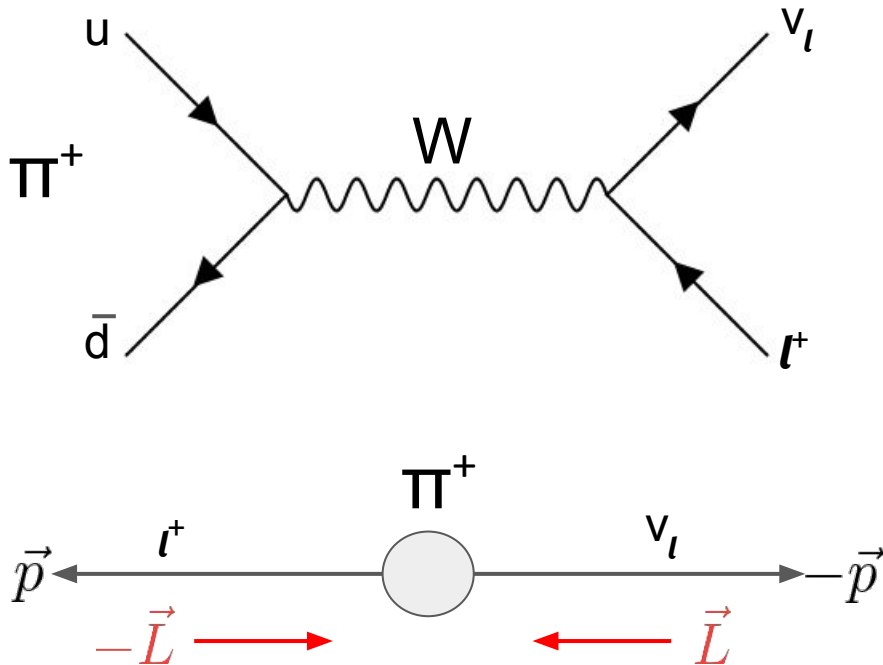
Helicity Suppression (Why is Muon Decay Most Likely?)

- We can write the LH (negative) helicity anti-particle state in the chiral basis:

$$v_\downarrow = \frac{A}{2}\left[\left(1 - \frac{p}{E+m}\right)v_R - \left(1 + \frac{p}{E+m}\right)v_L\right]$$

- We ignore the LH term (weak force only acts on the RH term), anti-particle's matrix element contribution:

$$\mathcal{M} \sim \frac{1}{2}\left(1 - \frac{p_l}{E_l + m_l}\right) \xrightarrow[m_\nu \to 0]{} \frac{m_l}{m_\pi + m_l}$$

- This effect ends up making the matrix element smaller → decay rate smaller

$$\Gamma \propto |\mathcal{M}|^2$$
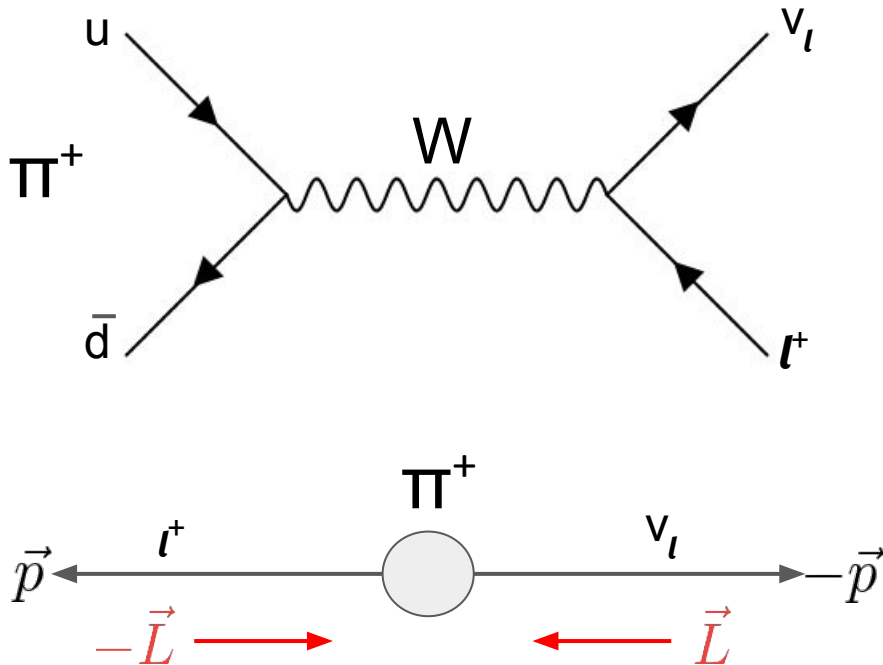
Lepton Universality
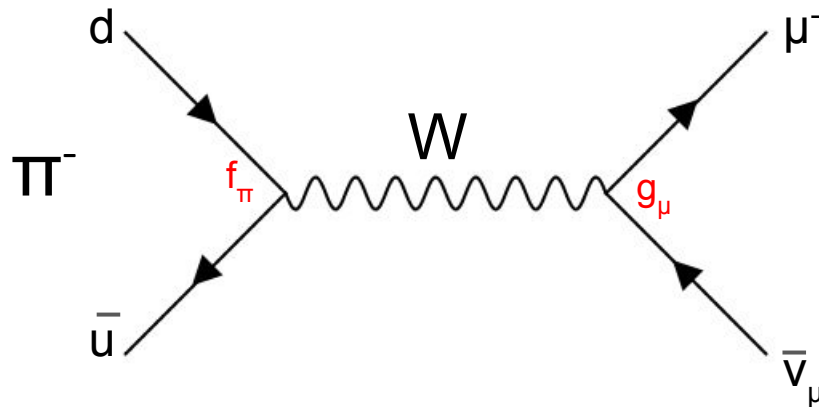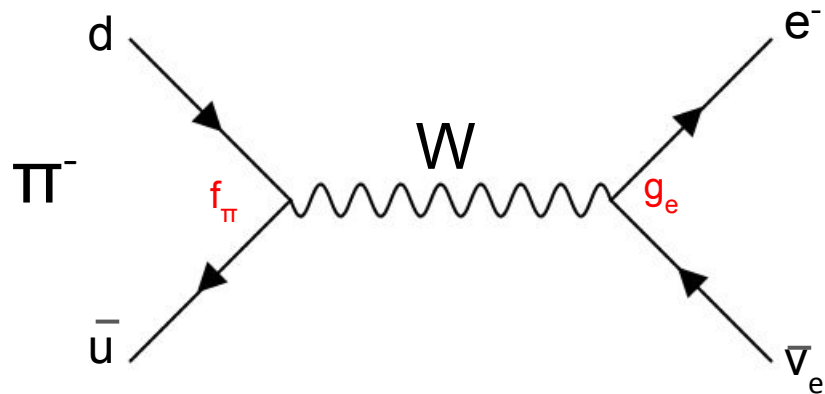
- States coupling strengths (vertices) $g_e = g_\mu = g_\tau$
- Using the Feynman rules for the weak interaction, we can approximate the matrix element

$$\mathcal{M}_{fi} = \left[\frac{g_W}{\sqrt{2}} \frac{1}{2} f_\pi p_\pi^\alpha \right] \cdot \left[\frac{g_{\alpha\beta}}{m_W^2} \right] \cdot \left[\frac{g_W}{\sqrt{2}} g_l \bar{u}(p_l) \gamma^\beta \frac{1}{2} (1 - \gamma^5) v(p_\nu) \right]$$

$$\underbrace{\hspace{3cm}}_{\text{Pion vertex}} \quad \underbrace{\hspace{2cm}}_{\substack{\text{W-boson} \\ \text{propagator}}} \quad \underbrace{\hspace{5cm}}_{\text{Lepton vertex}}$$

Lepton Universality

- After some "massaging" we can find the matrix element to be

$$\mathcal{M}_{fi} = \left(\frac{g_W}{2m_W}\right)^2 f_\pi g_l \cdot \sqrt{m_\pi^2 - m_l^2}$$

- Pion spin zero → no spin averaging needed, i.e.:

$$\langle |\mathcal{M}_{fi}|^2 \rangle = |\mathcal{M}_{fi}|^2 = \left(\frac{g_W}{2m_W}\right)^4 f_\pi^2 g_l^2 \cdot (m_\pi^2 - m_l^2)$$

- We can use the general formula for 2-body decay to to find the decay rate

$$\Gamma = \frac{p \langle |\mathcal{M}_{fi}|^2 \rangle}{8\pi m_\pi^2} = \frac{f_\pi^2}{16\pi^2 m_\pi^3} \left(\frac{g_W}{2m_W}\right)^4 \left[m_l g_l (m_\pi^2 - m_l^2)\right]^2$$

- Finally, we compute the branching ratio

$$\frac{\Gamma(\pi^- \to e^- \bar{\nu}_e)}{\Gamma(\pi^- \to \mu^- \bar{\nu}_\mu)} = \left(\frac{g_e}{g_\mu}\right)^2 \left[\frac{m_e(m_\pi^2 - m_e^2)}{m_\mu(m_\pi^2 - m_\mu^2)}\right]^2$$

Lepton Universality

$$\frac{\Gamma(\pi^- \to e^- \bar{\nu}_e)}{\Gamma(\pi^- \to \mu^- \bar{\nu}_\mu)} = \left(\frac{g_e}{g_\mu}\right)^2 \left[\frac{m_e(m_\pi^2 - m_e^2)}{m_\mu(m_\pi^2 - m_\mu^2)}\right]^2$$

- Lepton universality assumes $g_e = g_\mu$, so the first factor disappears

- Improving the branching ratio measurement and comparing to the theoretical value acts as a test of lepton universality

- Another test would consider pure leptonic decays, but such decays involving taus are too rare for high precision measurements

Branching Ratio $R_{e/\mu}$

- We can measure the branching ratio by measuring # of decays e and μ decays

$$R_{e/\mu} \equiv \frac{\Gamma(\pi^- \to e^- \bar{\nu}_e)}{\Gamma(\pi^- \to \mu^- \bar{\nu}_\mu)}$$

- Theoretical prediction is simple in first (and second) order
  - No f_π or CKM element V_{ud}

$$R^0_{e/\mu} = \left(\frac{g_e}{g_\mu}\right)^2 \left[\frac{m_e(m_\pi^2 - m_e^2)}{m_\mu(m_\pi^2 - m_\mu^2)}\right]^2$$

= 1 [in theory]

- 3rd order correction and beyond the pion structure becomes relevant

$$R^{(\text{theory})}_{e/\mu} = R^0_{e/\mu}\left(1 - \frac{3\alpha}{\pi}\ln\left(\frac{m_\mu}{m_e}\right) + \dots\right)$$

Citation: Testing Lepton Flavor Universality and CKM Unitarity with Rare Pion Decays in
the PIONEER experiment, PIONEER collab (pg. 6, arxiv: 2203.05505)

j.carlton@uky.edu

Current state of $R_{e/\mu}$

$$R_{e/\mu}^{exp} = 1.2327(23) \times 10^{-4} \text{ (PIENU collab)}$$

$$R^{theo} = 1.23524(15) \times 10^{-4}$$

- Consistent with each other

- Expect factor of ~10 precision improvement on experimental value from PIONEER
  - "Catches up" with theoretical uncertainty

j.carlton@uky.edu

Past Experimental Approach (PIENU)

- NaI has a long primary decay time
  - ~ 250 ns
- Event pileup forces the experiment to run at a low rate
  - ~70 kHz
- "inactive target", muons aren't tracked
- CsI Rings for shower leakage detection

j.carlton@uky.edu
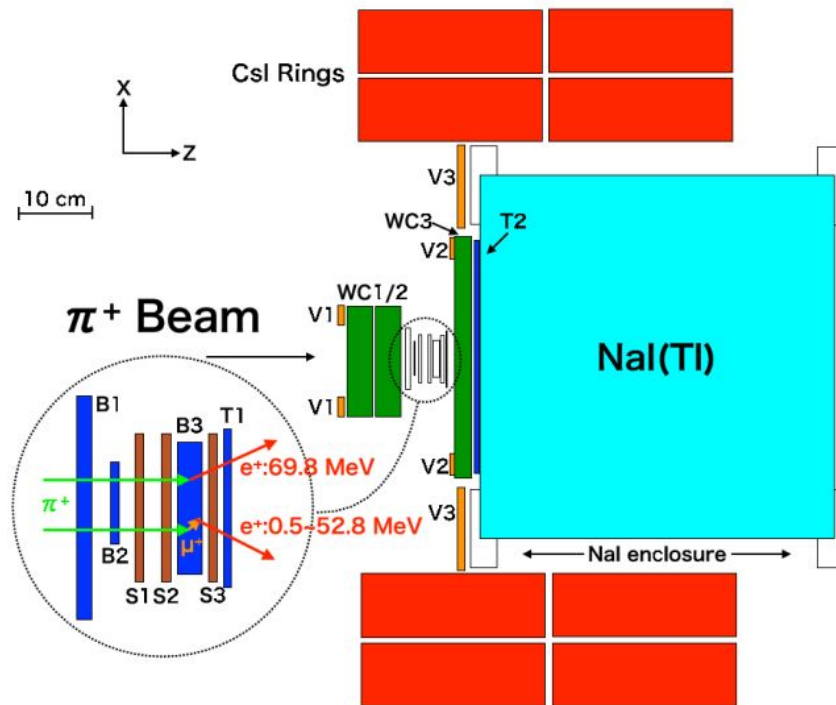
Common Pion Decay Channels

$\boxed{}$ = Most Common

Leptonic Decay

- $\pi^+ \rightarrow e^+ + \nu_e$

- $\pi^- \rightarrow e^- + \bar{\nu}_e$

- $\pi^+ \rightarrow \mu^+ + \nu_\mu$

- $\pi^- \rightarrow \mu^- + \bar{\nu}_\mu$

Beta Decay

- $\pi^+ \rightarrow \pi^0 + e^+ + \nu_e$

- $\pi^- \rightarrow \pi^0 + e^- + \bar{\nu}_e$

Photon Decay

- $\pi^0 \rightarrow \gamma + \gamma$

Dalitz Decay

- $\pi^0 \rightarrow \gamma + e^- + e^+$

Double-Dalitz Decay

- $\pi^0 \rightarrow e^- + e^+ + e^- + e^+$

Electrons

- $\pi^0 \rightarrow e^- + e^+$

[Note: Dalitz Decays are like photon decays, except the photon(s) are virtual and immediately decay into electron/positron pairs]

Naive Pion Decay, 2-body decay

- Without getting into details of QCD, we can treat this as a 3 particle decay
- We can use Fermi's golden rule:

$$d\Gamma = |\mathcal{M}|^2 \cdot \frac{1}{2\hbar m_a} \cdot \left[\frac{cd^3\mathbf{p}_b^2}{(2\pi)^3 2E_b} \cdot \frac{cd^3\mathbf{p}_c^2}{(2\pi)^3 2E_c} \right] \cdot (2\pi)^4 \delta^4(p_a - p_b - p_c)$$

- After integration in the COM frame we find:

$$\Gamma = \frac{|\mathbf{p}|}{8\pi\hbar m_a^2 c} |\mathcal{M}|^2$$
$$\text{where } \mathbf{p} = \mathbf{p}_b = -\mathbf{p}_c$$

- → Γ ∝ p (not correct)
  - Details hidden in matrix element

j.carlton@uky.edu
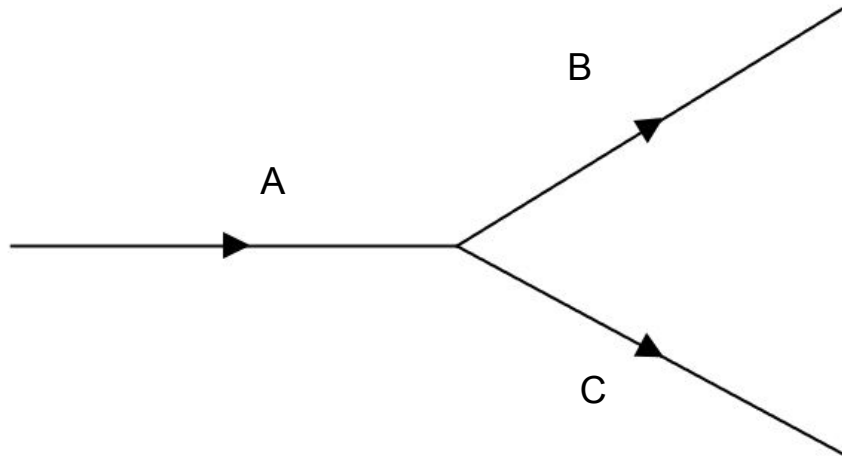
Why Massless → Chirality States ~ Helicity States

- Massless → moves at c

- Moves at c → cannot reverse particle direction with Lorentz boost → helicity is Lorentz Invariant

- Chirality is a property of a particle, always Lorentz invariant! → helicity and chirality agree in direction in all inertial reference frames

$(\gamma^\mu p_\mu - m)u(p) = 0$ [Dirac Equation]

$\implies \begin{pmatrix} -mI_{2\times2} & \sigma \cdot p \\ \bar\sigma \cdot p & -mI_{2\times2} \end{pmatrix} \begin{pmatrix} u_L \\ u_R \end{pmatrix} = 0$ [Chiral States]

$\implies \begin{cases} (\sigma \cdot p)u_R - mu_L = 0 \\ (\bar\sigma \cdot p)u_L - mu_R = 0 \end{cases}$

$m \to 0 \implies \begin{cases} (p_0 - \boldsymbol{\sigma} \cdot \mathbf{p})u_R = 0 \\ (p_0 + \boldsymbol{\sigma} \cdot \mathbf{p})u_L = 0 \end{cases}$

$\implies \begin{cases} \frac{\boldsymbol{\sigma} \cdot \mathbf{p}}{|\mathbf{p}|}u_R = u_R \\ \frac{\boldsymbol{\sigma} \cdot \mathbf{p}}{|\mathbf{p}|}u_L = -u_L \end{cases}$

$\hat{h} = \frac{\mathbf{S} \cdot \mathbf{p}}{|\mathbf{p}|} = \frac{1}{2}\frac{\boldsymbol{\sigma} \cdot \mathbf{p}}{|\mathbf{p}|}$ [Helicity operator]

$\implies \begin{cases} \hat{h}u_R = \frac{1}{2}u_R \\ \hat{h}u_L = -\frac{1}{2}u_L \end{cases}$ [Chiral states are eigenstates of helicity operator]

LH (negative) helicity spinor to chiral components

An negative helicity antiparticle can be written as

$$v_\downarrow = \sqrt{E+m} \begin{pmatrix} \frac{|\mathbf{p}|}{E+m}\cos(\frac{\theta}{2}) \\ \frac{|\mathbf{p}|}{E+m}\sin(\frac{\theta}{2})e^{i\phi} \\ \cos(\frac{\theta}{2}) \\ \sin(\frac{\theta}{2})e^{i\phi} \end{pmatrix}$$

Where (θ,φ) define the direction of the momentum. Without loss of generality, assume the momentum is in the z direction

$$v_\downarrow = \sqrt{E+m} \begin{pmatrix} \frac{|\mathbf{p}|}{E+m} \\ \frac{|\mathbf{p}|}{E+m} \\ 1 \\ 1 \end{pmatrix} \equiv A \begin{pmatrix} \tau\xi_R \\ \xi_R \end{pmatrix}$$

LH (negative) helicity spinor to chiral components

We can use the chiral projection operations to project this helicity state to chiral state

$$v_\downarrow = P_L v_\downarrow + P_R v_\downarrow$$

$$P_R = \frac{I_{4\times 4} + \gamma^5}{2} = \begin{pmatrix} I_{2\times 2} & I_{2\times 2} \\ I_{2\times 2} & I_{2\times 2} \end{pmatrix}$$

$$P_L = \frac{I_{4\times 4} - \gamma^5}{2} = \begin{pmatrix} I_{2\times 2} & -I_{2\times 2} \\ -I_{2\times 2} & I_{2\times 2} \end{pmatrix}$$

$$v_\downarrow = \frac{A}{2}\left[(1-\tau)\begin{pmatrix} -\xi_R \\ \xi_R \end{pmatrix} + (1+\tau)\begin{pmatrix} \xi_R \\ \xi_R \end{pmatrix} \right] \equiv \frac{A}{2}(1-\tau)v_R - \frac{A}{2}(1+\tau)v_L$$

Where the left and right chiral anti-particle states are defined by

$$P_L v_R = v_R \text{ and } P_R v_L = v_L$$

LH (negative) helicity spinor to chiral components

Looking at the chiral projection of a negative helicity state, we can see in general there are left **and** right chiral components, so the weak force **can** act on a LH (negative) anti-particle helicity state

$$v_\downarrow = \frac{A}{2}\left[\left(1 - \frac{p}{E+m}\right)v_R - \left(1 + \frac{p}{E+m}\right)v_L\right]$$

It should also be clear as m→0, the LH (negative) helicity state coincides with the LH chiral state.

This means W boson decay to two massless leptons is forbidden! One of the particles must have the wrong chirality, and thus low mass decays will be suppressed.

Matrix Element Details

$$\mathcal{M}_{fi} = \left[\frac{g_W}{\sqrt{2}} \frac{1}{2} f_\pi p_\pi^\alpha \right] \cdot \left[\frac{g_{\alpha\beta}}{m_W^2} \right] \cdot \left[\frac{g_W}{\sqrt{2}} g_l \bar{u}(p_l) \gamma^\beta \frac{1}{2} (1 - \gamma^5) v(p_\nu) \right]$$

Move to pion rest frame so only $p^0 = m_\pi$ remains:

$$\mathcal{M}_{fi} = \frac{g_W^2 f_\pi g_l}{4 m_W^2} m_\pi \bar{u}(p_l) \gamma^0 \frac{1}{2} (1 - \gamma^5) v(p_\nu)$$

Using the identity: $\bar{u}(p_l)\gamma^0 = u^\dagger(p_l)\gamma^0\gamma^0 = u^\dagger(p_l) I_{4\times4} = u^\dagger(p_l)$

$$\mathcal{M}_{fi} = \frac{g_W^2 f_\pi g_l}{4 m_W^2} m_\pi u^\dagger(p_l) \frac{1}{2} (1 - \gamma^5) v(p_\nu)$$

Matrix Element Details

For a neutrino m << E so helicity eigenstate is essentially the chiral eigenstate:

$$\frac{1}{2}(1 - \gamma^5)v(p_\nu) = v_\uparrow(p_\nu) \implies \mathcal{M}_{fi} = \frac{g_W^2 f_\pi g_l}{4m_W^2} m_\pi u^\dagger(p_l)v_\uparrow(p_\nu)$$

By letting the lepton go in the z-direction we can write:

$$u(p_l) = u_\uparrow(p_l) + u_\downarrow(p_l) = \sqrt{E_l + m_l}\left[\begin{pmatrix} 1 \\ 0 \\ \frac{p}{E_l+m_l} \\ 0 \end{pmatrix} + \begin{pmatrix} 0 \\ 1 \\ 0 \\ \frac{-p}{E_l+m_l} \end{pmatrix}\right] \text{ and } v(p_\mu) = v_\uparrow(p_\mu) = \sqrt{p}\begin{pmatrix} 1 \\ 0 \\ -1 \\ 0 \end{pmatrix}$$

Negative helicity lepton down state disappears when "dotted" with the neutrino state:

$$\mathcal{M}_{fi} = \frac{g_W^2 f_\pi g_l}{4m_W^2} m_\pi \sqrt{E_l + m_l}\sqrt{p}\left(1 - \frac{p}{E_l + m_l}\right)$$

Matrix Element Details

$$\mathcal{M}_{fi} = \frac{g_W^2 f_\pi g_l}{4m_W^2} m_\pi \sqrt{E_l + m_l} \sqrt{p} \left(1 - \frac{p}{E_l + m_l} \right)$$

We can re-write E_l and p in the limit where the neutrino mass is zero:

$$E_l = \frac{m_\pi^2 + m_l^2}{2m_\pi} \text{ and } p_l = \frac{m_\pi^2 - m_l^2}{2m_\pi}$$

$$\implies \mathcal{M}_{fi} = \frac{g_W^2 f_\pi g_l}{4m_W^2} m_\pi \cdot \frac{m_\pi + m_l}{\sqrt{2m_\pi}} \cdot \left(\frac{m_\pi^2 - m_l^2}{2m_\pi} \right)^{\frac{1}{2}} \cdot \frac{2m_l}{m_\pi + m_l}$$

$$\implies \mathcal{M}_{fi} = \frac{g_W^2 f_\pi g_l}{4m_W^2} \cdot m_l (m_\pi^2 - m_l^2)^{\frac{1}{2}}$$

Lepton Universality

Note: $x^2 = 1 + 2(x - 1) + \mathcal{O}(x^2)$

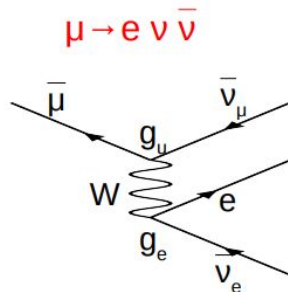Let: $\left(\dfrac{g_e}{g_\mu}\right) \equiv (1 + \Delta_{\frac{g_e}{g_\mu}}) \equiv x$

$$R_{e/\mu} = \frac{\Gamma(\pi^- \to e^- \bar{\nu}_e)}{\Gamma(\pi^- \to \mu^- \bar{\nu}_\mu)} \approx (1 + 2\Delta_{\frac{g_e}{g_\mu}}) \left[\frac{m_e(m_\pi^2 - m_e^2)}{m_\mu(m_\pi^2 - m_\mu^2)}\right]^2$$

Let: $\Delta R_{e/\mu} = R_{e/\mu} - \left(R_{e/\mu}\right)_{\text{theory}}$

$$\boxed{\frac{\Delta R_{e/\mu}}{\left(R_{e/\mu}\right)_{\text{theory}}} = 2\Delta_{\frac{g_e}{g_\mu}}} \implies$$

Small discrepency in g_e/g_μ and 1 can cause twice as big discrepency in measured $R_{e/\mu}$ and theory $R_{e/\mu}$

j.carlton@uky.edu

Another Test for Lepton Universality
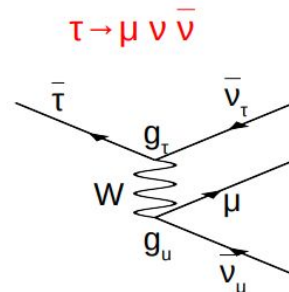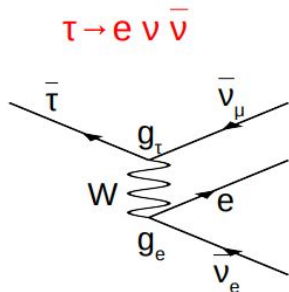
Fermi constant, $G_F = g^2 / 4\sqrt{2}M_W^2$

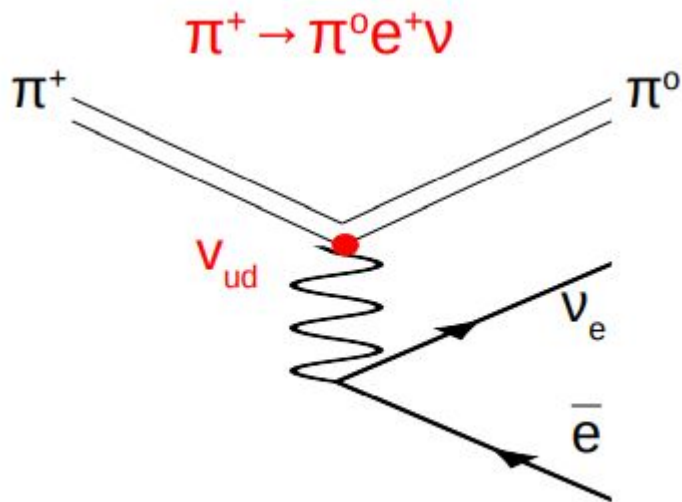$G_{\mu e} = 1.166\ 378\ 7(6) \times 10^{-5}$ GeV^{-2} (0.5 ppm)

$G_{\tau\mu} = 1.1665(28) \times 10^{-5}$ GeV^{-2} (0.2%)

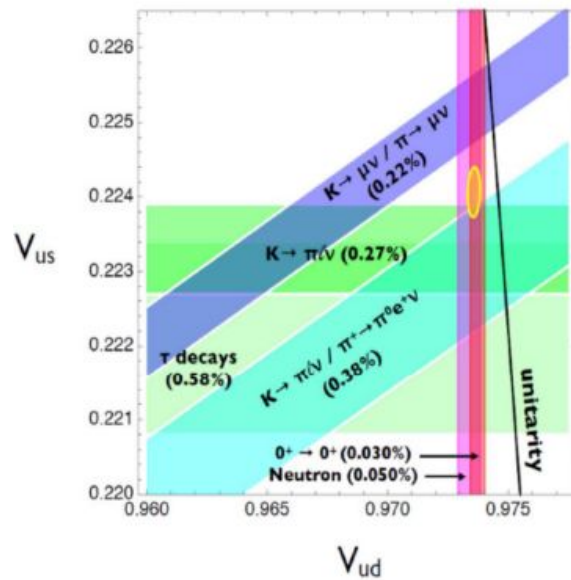$G_{\tau e} = 1.1665(28) \times 10^{-5}$ GeV^{-2} (0.2%)

weak coupling, g

$g_e : g_\mu : g_\tau$ 1 : 1.0011(24) : 1.0006(24)

j.carlton@uky.edu

CKM Unitary Test

arXiv:2203.05505

- Pion beta decay gives a precision measurement of V_{ud}
- These decays are lower rate than $\pi \to e\nu_e$ and $\pi \to \mu\nu_\mu$
- Experimental measurements do not agree

j.carlton@uky.edu

Some Information about LXe and NaI

- LXe has singlet and triplet state decay constants:
  - τ_S = 4.3 ± 0.6 ns
  - τ_T = $26.9^{+0.7}_{-1.1}$ ns
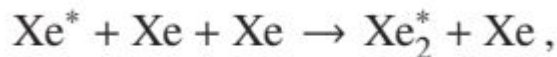- LXe light yield:
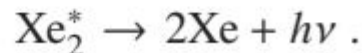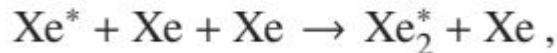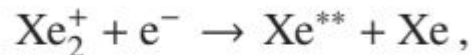 - ~29 photons/keV at room temp

- NaI decay constant:
  - ~ 250 ns
- NaI light yield:
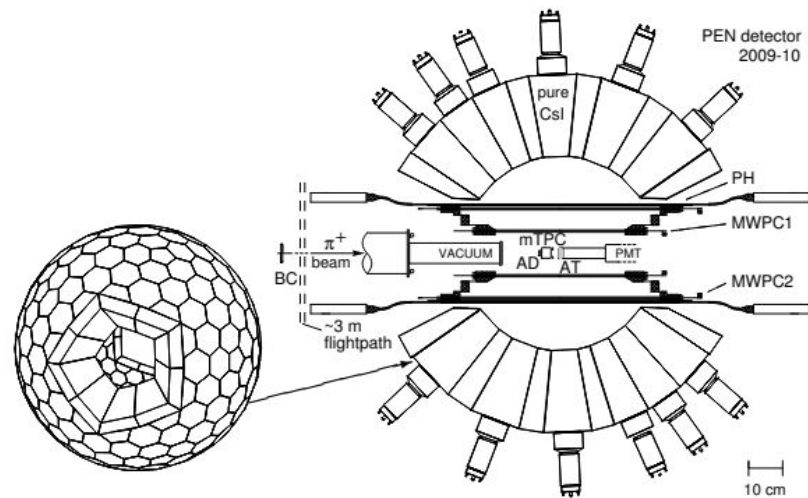 - 38 photons/keV at room temp

Scintillation from excited Xe (Xe*):

$$Xe^* + Xe + Xe \rightarrow Xe_2^* + Xe,$$

$$Xe_2^* \rightarrow 2Xe + h\nu.$$

Scintillation from ionized Xe (Xe⁺):

$$Xe^+ + Xe \rightarrow Xe_2^+,$$

$$Xe_2^+ + e^- \rightarrow Xe^{**} + Xe,$$

$$Xe^{**} \rightarrow Xe^* + heat,$$

$$Xe^* + Xe + Xe \rightarrow Xe_2^* + Xe,$$

$$Xe_2^* \rightarrow 2Xe + h\nu.$$

j.carlton@uky.edu
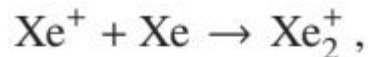
PEN

- ## Similar to PIENU
  - ### Segmented
  - ### Better timing

- ## Many channels of pure CSI
  - ### 240 channels

- ## Active target

PEN detector
2009-10

pure
CsI

PH

MWPC1

π^+ beam

VACUUM

mTPC

AD   AT

PMT

MWPC2

BC

~3 m
flightpath

10 cm

j.carlton@uky.edu

More ATAR details

- Pion and muon decays deposit energy into ATAR
- Allow event types to be distinguished
- Muons decaying in flight can boost positron energy past 53 MeV (big issue!)
  - ATAR can give information to rebuild event, and correctly classify a muon decay

arxiv: 2203.01981

j.carlton@uky.edu
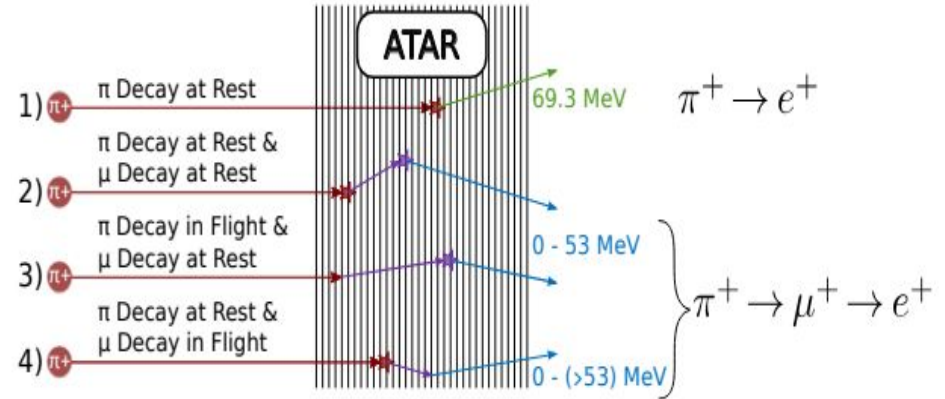
Another Calorimeter 3D Render (Liquid Xenon)

1.5m
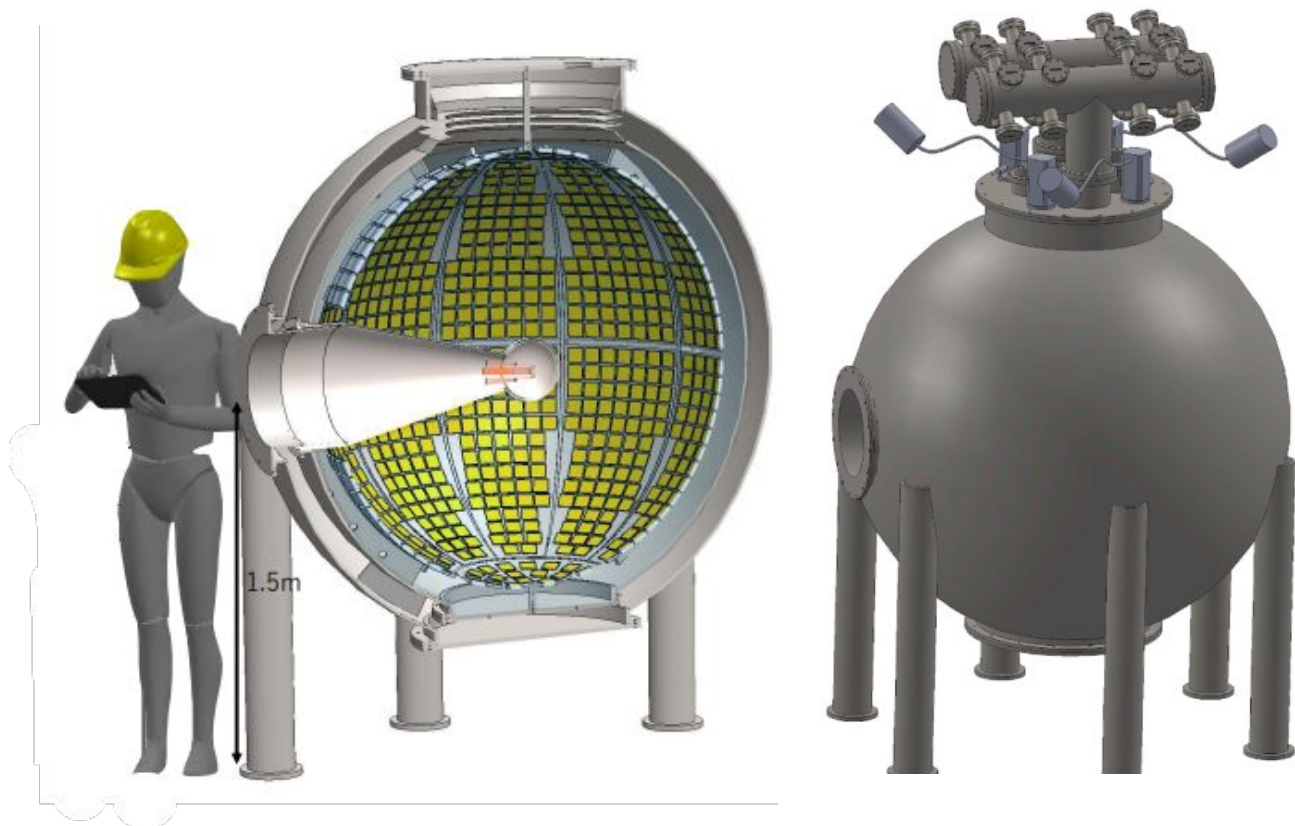
Electronics and Data Rates

Initialism Cheatsheet

Initialism	Meaning	Example
10GbE	10 Gigabit Ethernet	
FPGA	Field Programmable Gate Array	
FMC	FPGA Mezzanine Card	FC7 SFP Interface
CPU	Central Processing Unit	Intel Core i7-12700K
GPU	Graphics Processing Unit	NVIDIA A5000
μTCA (uTCA)	Micro Telecommunications Computing Architecture	
WFD	Waveform Digitizer	WFD5
FC	Flexible Controller	FC7
AMC	Advanced Mezzanine Card	AMC13 (also FC7 and WFD5)
MCH	MicroTCA Carrier Hub	
DDR	Double Data Rate	DDR3, DDR4 (RAM)
PCIe	Peripheral Component Interconnect Express	PCIe2, PCIe3, ...
TTC	Timing, Trigger, and Control	
UART	Universal Asynchronous Receiver-Transmitter	

Hardware - Conceptual Diagram

- Differential signal into WFD5 (Waveform Digitizer)
- Trigger signal into FC7 (Flexible Controller)
- AMC13 (Advanced Mezzanine Card) gathers data, sends over 10GbE (10 Gigabit Ethernet) to desktop
- MCH (MicroTCA Carrier Hub) facilitates Desktop↔Crate communication over 1GbE
- Desktop CPU handles event processing
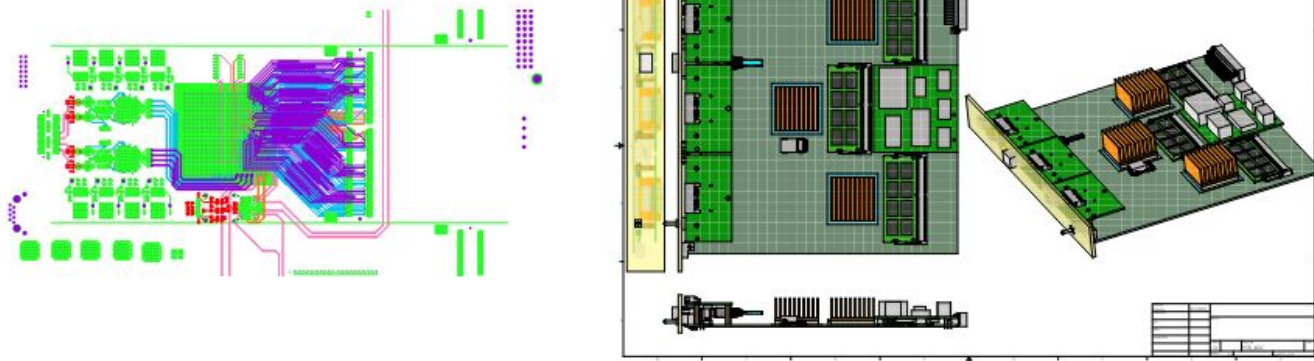- Meinberg gives trigger timestamp to computer
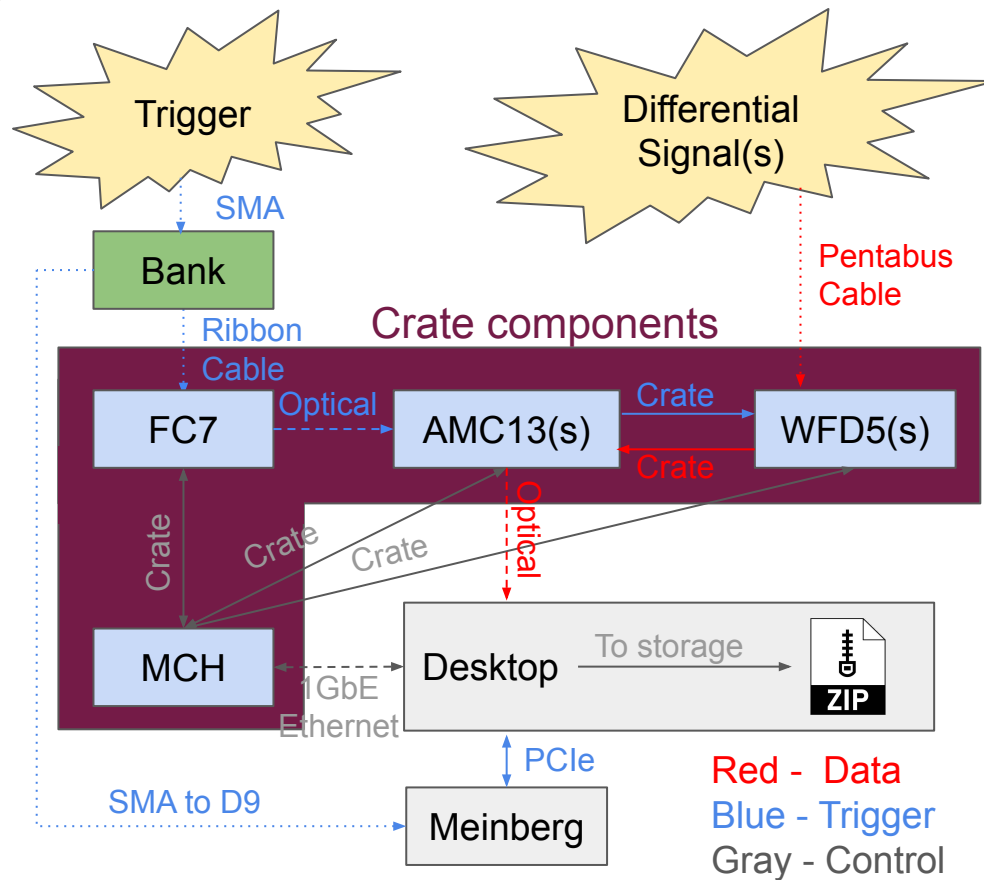
# Hardware - Unlabeled Picture
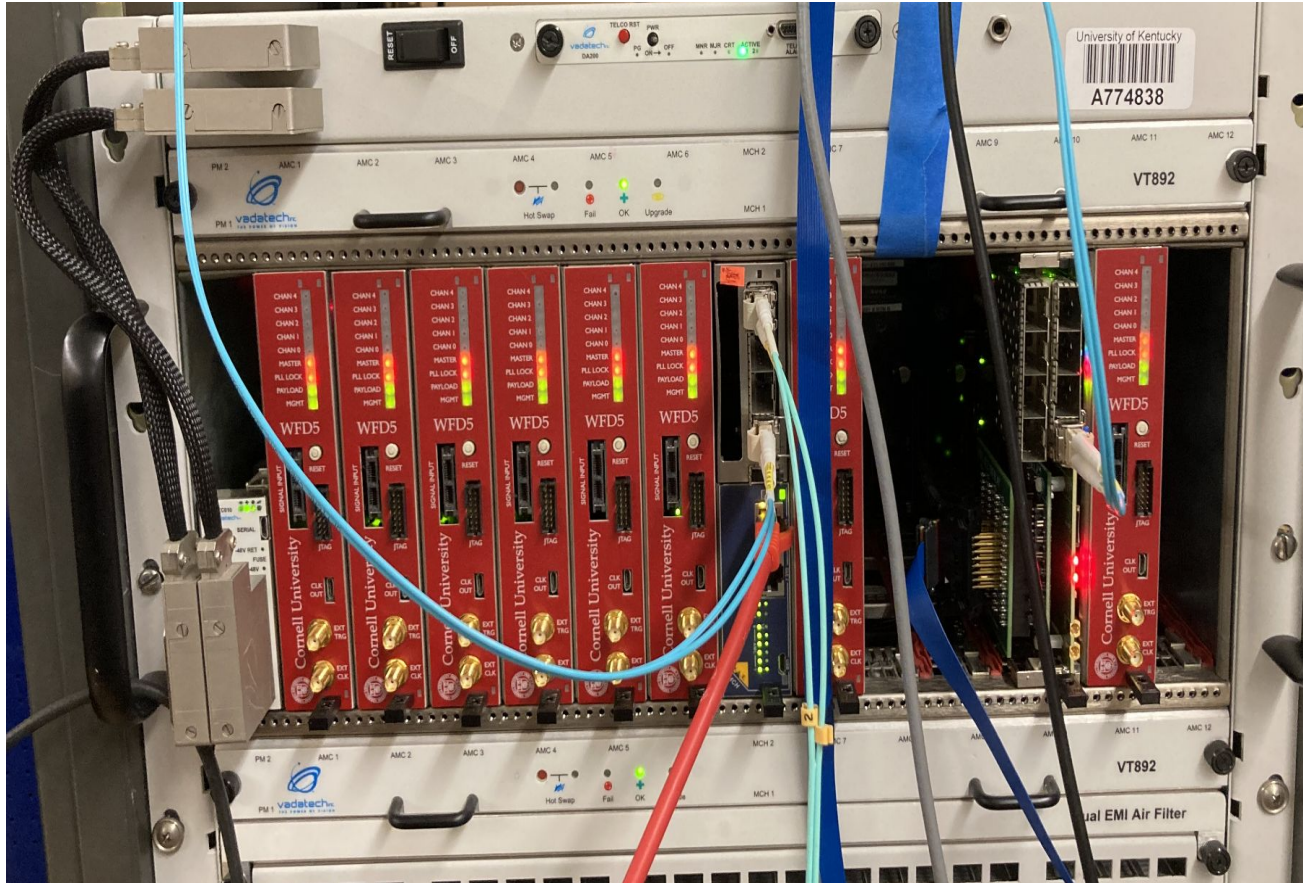
PIONEER DAQ (in a nascent state)

- ## PIONEER DAQ
  - In nascent development state
  - Design catered to PIONEER full experiment necessities

PIONEER ADC schematic drawings

"Older" PCIe DMA Transfer Rates are Better

- Transfer rates using block ram in a computer with an older OS (CentOS7)
- There is a leveling off effect at high transfer sizes
- XDMA driver by Xilinx seems to changes with kernel version, causing performance differences

Transfer Speed Vs. Transfer Size

j.carlton@uky.edu
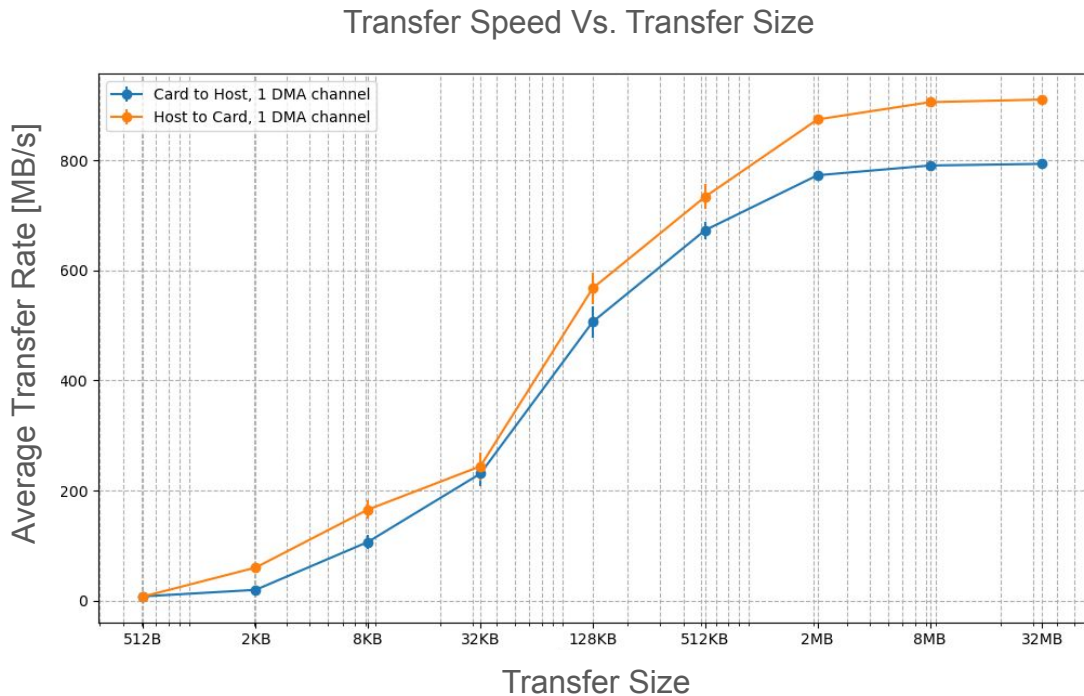
Data Rates (CALO data rates LXe/LYSO dependant)

arXiv:2203.01981

triggers	prescale	range TR(ns)	rate (kHz)	CALO ΔT(ns)	chan	MB/s	ATAR digitizer ΔT(ns)	chan	MB/s	ATAR high thres chan	MB/s
PI	1000	-300,700	0.3	200	1000	120	30	66	2.4	20	0.012
CaloH	1	-300,700	0.1	200	1000	40	30	66	0.8	20	0.004
TRACK	50	-300,700	3.4	200	1000	1360	30	66	27	20	0.014
PROMPT	1	2,32	5	200	1000	2000	30	66	40	20	0.2

- PIONEER DAQ expects data rate of ~**3.5GB/s**
- Considering running time, this is ~**35,000 TB/year**
- How do we compress this in real time?
  - Fit data, store fit parameters
  - Compress and store residuals, throw some out
  - Graphics Processing Units (GPUs) used for this operation

PSI Data

j.carlton@uky.edu

LYSO Information

- LYSO – lutetium–yttrium oxyorthosilicate
  - Lutetium (73%), Oxygen (18%), Silicon (6%), Yttrium (3%), and a Cerium scintillation dopant (~ 0%)
- Density = **7.4 g/cm^3**
- X_0 = **1.14 cm** = "Radiation length" = distance for an electron's energy to be reduced by a factor of 1/e
- R_M = **2.07 cm** = "Moliére radius" = radius of a cylinder containing on average 90% of the shower's energy deposition
- Light Yield = **30,000 photons/MeV**
- Scintillating decay time = **40 ns**

LYSO All Sides Polished
Size: 3mm x 3mm x 20mm

j.carlton@uky.edu
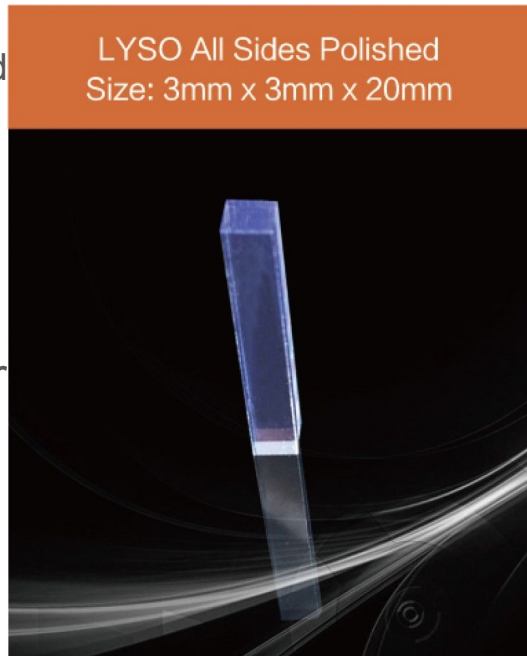
Energy Resolution Definition

- Energy resolution = ΔE/E
  - E is the peak energy
  - ΔE is the width of the peak
- Gaussian fit around the peak
  - a "crystal ball" fit is used here
  - Gaussian around center, x^{-n} on "sides" where n is a parameter
  - Gaussian parameter σ used for ΔE
- In this case, p4 = **E = 70.80 ± 0.02 MeV**
- p3 = **ΔE = 1.098 ± 0.014 MeV**
- ΔE/E = 0.0155 = 1.55%

70 MeV -- 1.55% Energy Resolution

htotE	
Entries	42779
Mean	6.7677e+1
Std Dev	4.8915e+0
χ^2 / ndf	522.6 / 514
p0	481.9 ± 3.6
p1	0.2854 ± 0.0064
p2	21.73 ± 3.58
p3	1.098 ± 0.014
p4	70.80 ± 0.02
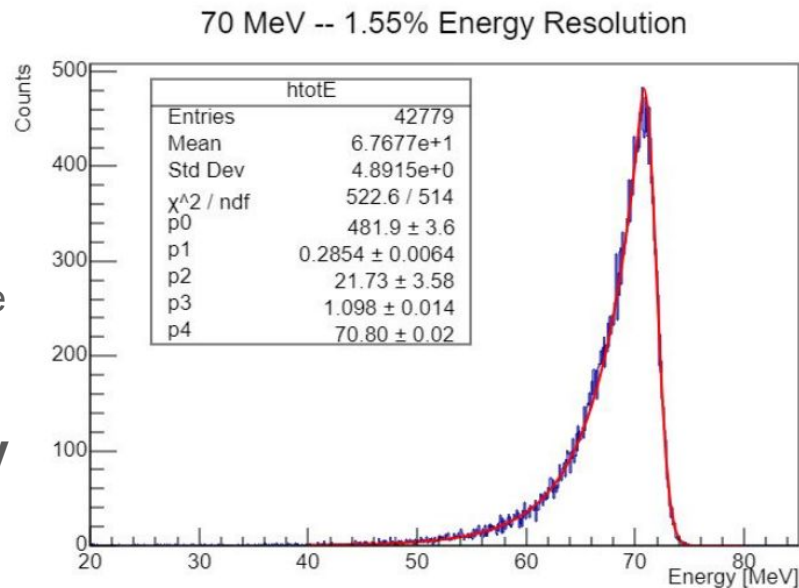
Timing Resolution Definition

- Use the strongest signal in an event as reference signal.
  - t_0 = time of peak
- In the same event find all crystal peaks t_i
  - Only use peaks above some energy threshold
- $\Delta t = t_0 - t_i$
  - The width of a gaussian fit to a histogram of all such measurements gives the timing resolution

j.carlton@uky.edu
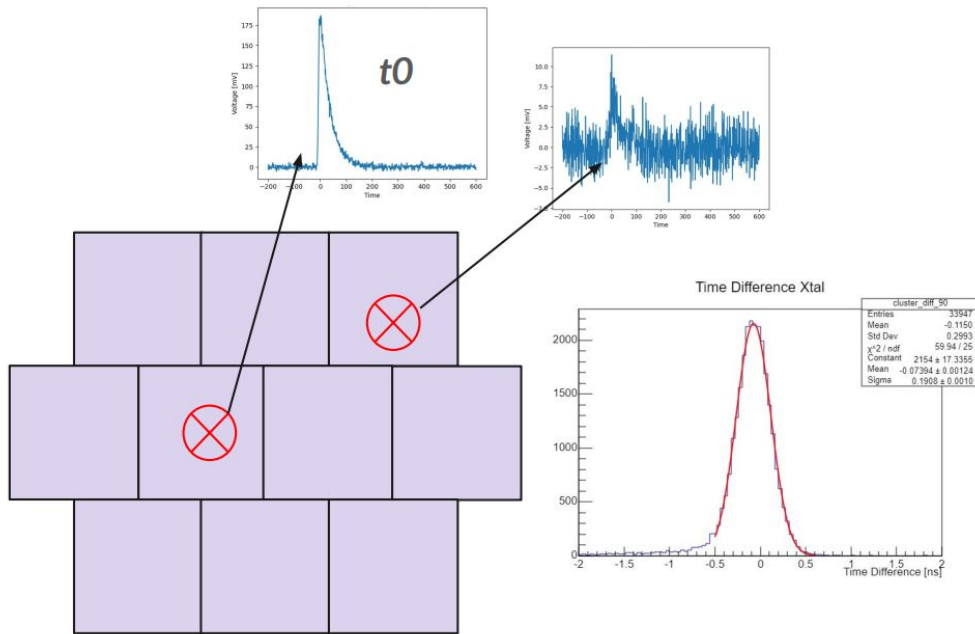
Results - Timing Resolution

- Timing resolution for 70 MeV events expected to be about 122.5 ps
- This measurement was largely influenced by noise from incorrect high voltage during test beam
  - Using a system of synchronized LEDs, clean, simultaneous signals were generated at UW
  - Improved timing resolution to about 60 ps
  - About that same as LXe

j.carlton@uky.edu
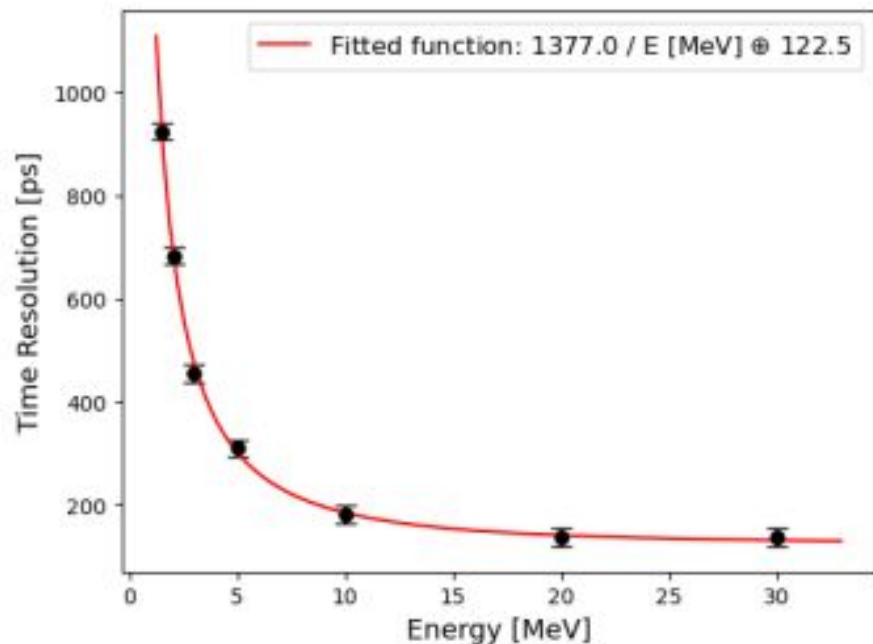
Results - Energy Resolution

- Energy resolution is uniform near the center of the lyso array

- Towards the edges the energy resolution decreases due to leakage
  - In this case, into the NaI array
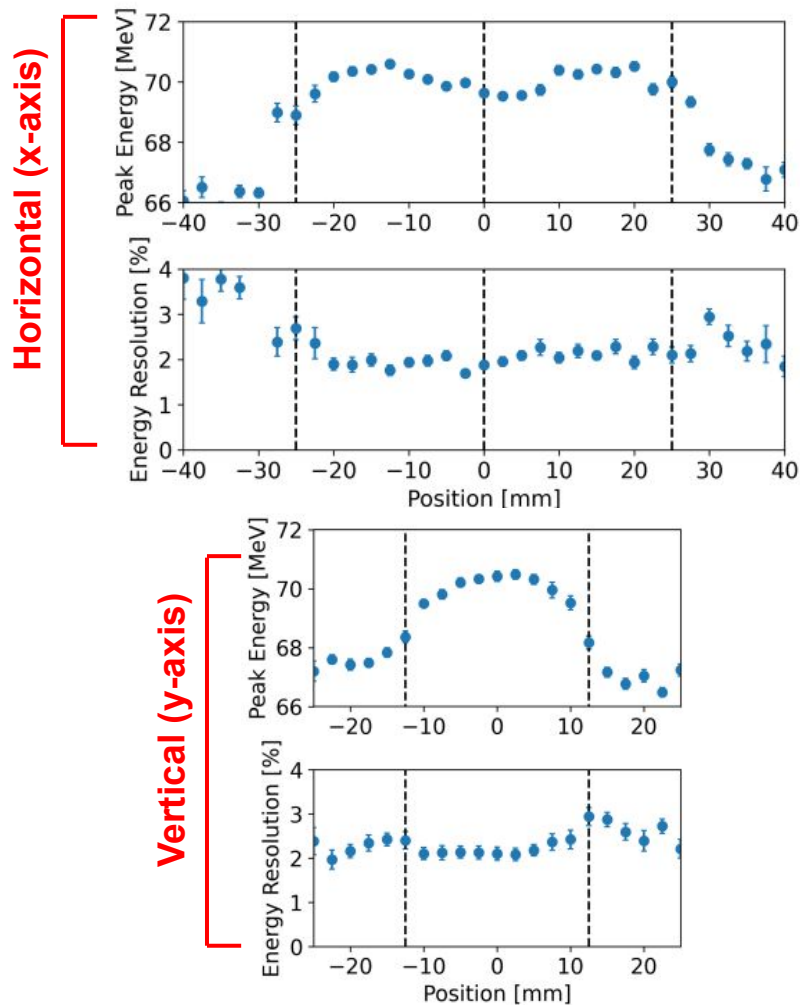
Compression and Entropy

Data Set

- PSI Test beam, Run 1887
- 70 MeV/c centered on LYSO crystal 4.
- The data only includes lyso channels (no NaI for instance)
- More details on that run are in this elog (https://maxwell.npl.washington.edu/elog/pienuxe/R23/124)
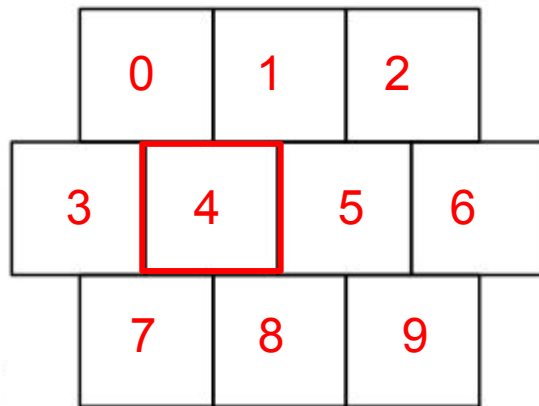
LYSO traces

- Select only LYSO channels and traces with a signal

- No pedestal subtraction, fitting, etc. (yet)
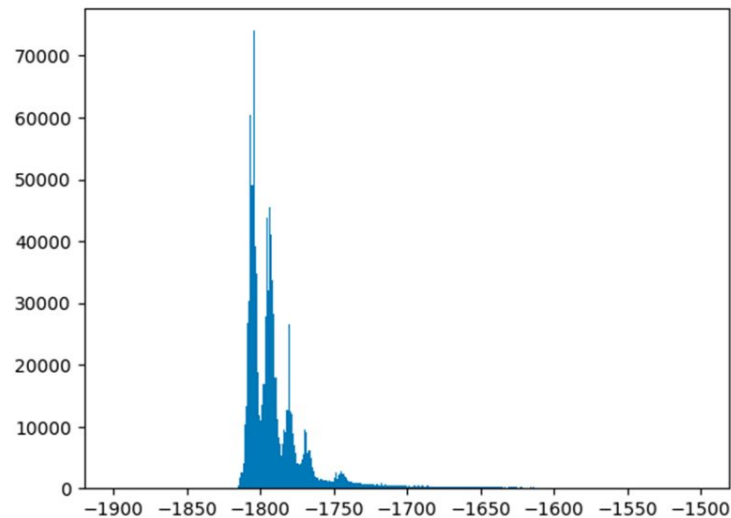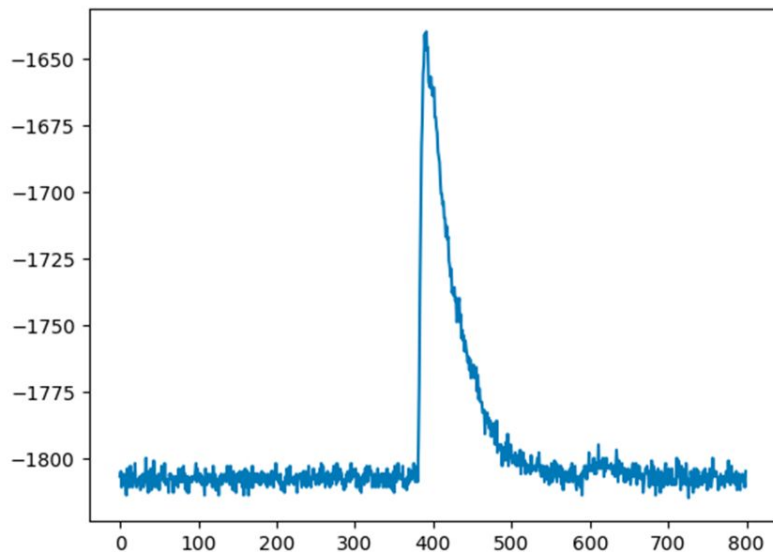
Entropy and Lossless Compression

- For lossless compression, the best possible compression rate is the entropy rate

- To first order, the entropy of an entire trace is:

$$H(X_1, ..., X_n) = - \sum_{\text{traces}} p(X_1, ..., X_n) \log_2(p(X_1, ..., X_n))$$

- X_i is the random variable for the ADC value of the ith sample in the trace with n samples

- If we assume X_i independent, then

$$H(X_1, ..., X_n) = H(X_1) + ... + H(X_n)$$

- By transforming ($X_i \rightarrow$ fit residuals), X_i becomes approximately independent

Higher Order Entropy Estimations

- Assume we have N characters (traces) in our alphabet (data set)

- **Zero order:** each character in alphabet is statistically independent

$$H = \log_2(N)$$

- **First order:** each character in alphabet is statistically independent, p_i is the probability of that character to occur

$$H = -\sum_{i=1}^{N} p_i \log_2(p_i)$$

- **Second order:** $P_{j|i}$ is correlation between subsequent characters

$$H = -\sum_{i=1}^{N} p_i \sum_{j=1}^{N} P_{j|i} \log_2(P_{j|i})$$

- **General Model (impractical):** B_n represents the first n characters

$$H = \lim_{n\to\infty} \left[-\frac{1}{n} \sum p(B_n) \log_2(B_n) \right]$$

Joint Entropy, Mutual Information

$$H(X_1, ..., X_n) \leq H(X_1) + ... + H(X_n)$$

Equality only holds if

$$X_1, ..., X_n \text{ are mutually statistically independent}$$

This means if

$$I(X_1, X_2) = H(X_1) + H(X_2) - H(X, Y) = 0$$

Then we must have X_1 and X_2 be statistically independent

j.carlton@uky.edu

Joint entropy for Independent Variables Proof

Statement:

$$H(X_1, ..., X_n) = \sum_{i=1}^{n} H(X_i)$$

Proof (part 1):

$$H(X_1, ..., X_n) = - \sum_{x_1, ..., x_n} P(x_1, ..., x_n) \log_2(P(x_1, ..., x_n))$$

$$= - \sum_{x_1, ..., x_n} P(x_1)...P(x_n) \left(\log_2(P(x_1)) + ... + \log_2(P(x_n)) \right)$$

(Note: I am lazy, each P(x$_i$) represents a different pdf in general)

j.carlton@uky.edu

Joint entropy for Independent Variables Proof

Proof (part 2):

$$H(X_1, ..., X_n) = -\left(\sum_{x_1} P(x_1) \log_2(P(x_1))\right)\left(\sum_{x_2} P(x_2) \cdot ... \cdot \sum_{x_n} P(x_n)\right)$$

$$- ...$$

$$-\left(\sum_{x_1} P(x_1) \cdot ... \cdot \sum_{x_{n-1}} P(x_{n-1})\right)\left(\sum_{x_n} P(x_n) \log_2(P(x_n))\right)$$

$$\text{Note } \sum_{x_i} P(x_i) = 1 \text{ and } \sum_{x_1} P(x_i) \log_2(P(x_i)) = H(X_i)$$

$$= H(X_1) + ... + H(X_n) \ \blacksquare$$

Entropy estimation

- Average entropy per bit: 5.22 bits / sample (compare to 16 bits for a short)

- Samples near waveform edge have lower entropy

- Samples near middle have higher entropy, due to the pulses

- Entropy is nonzero b/c the waveforms are **not** identical: difference pedestals, different pulse sizes

Entropy vs. sample number
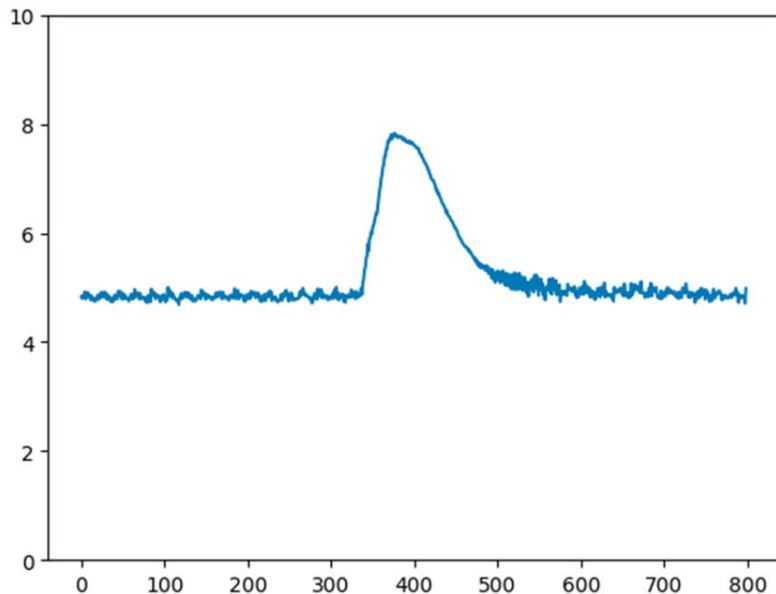
Pedestal subtracted
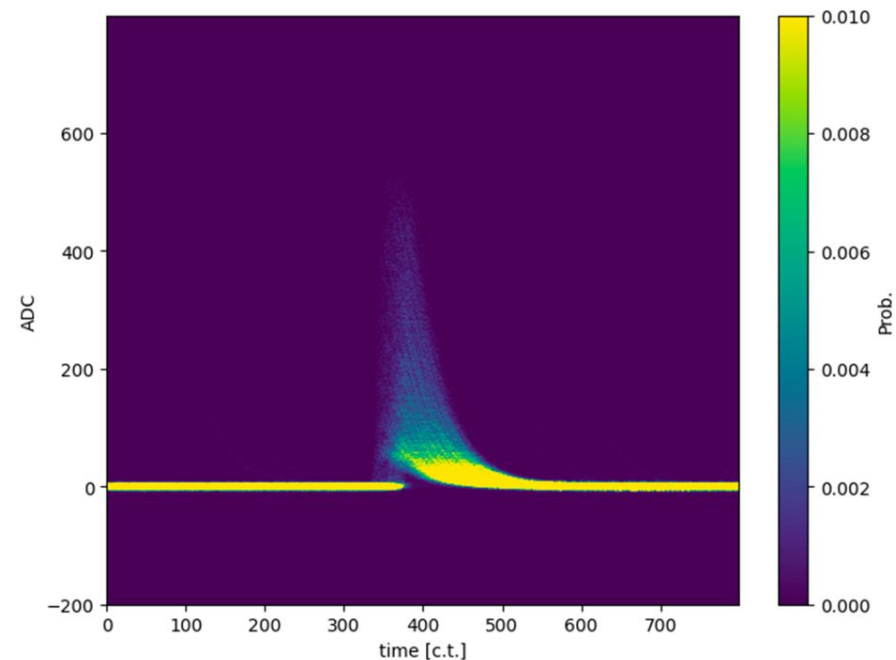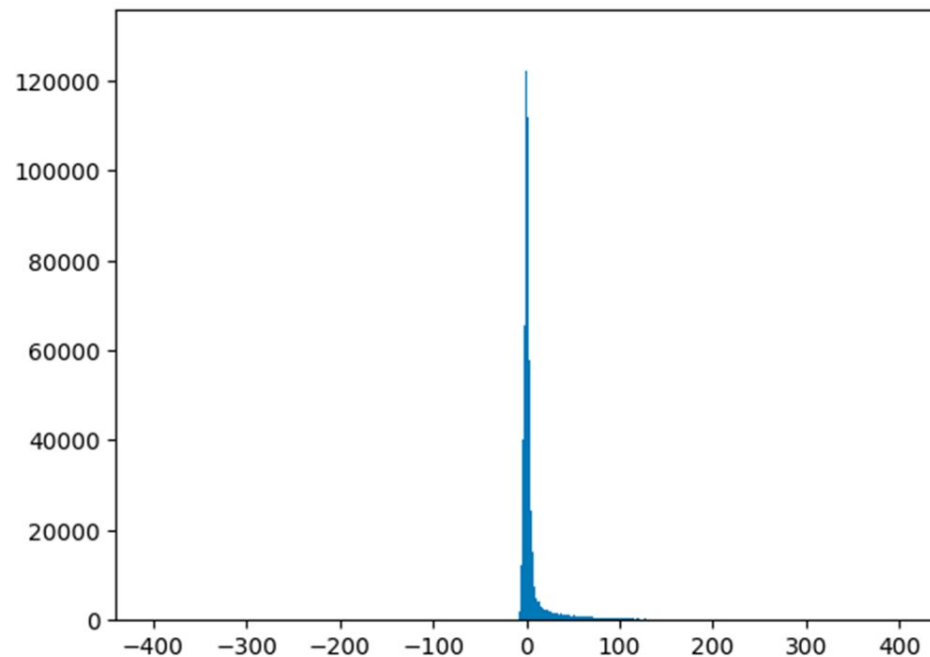
Entropy estimation
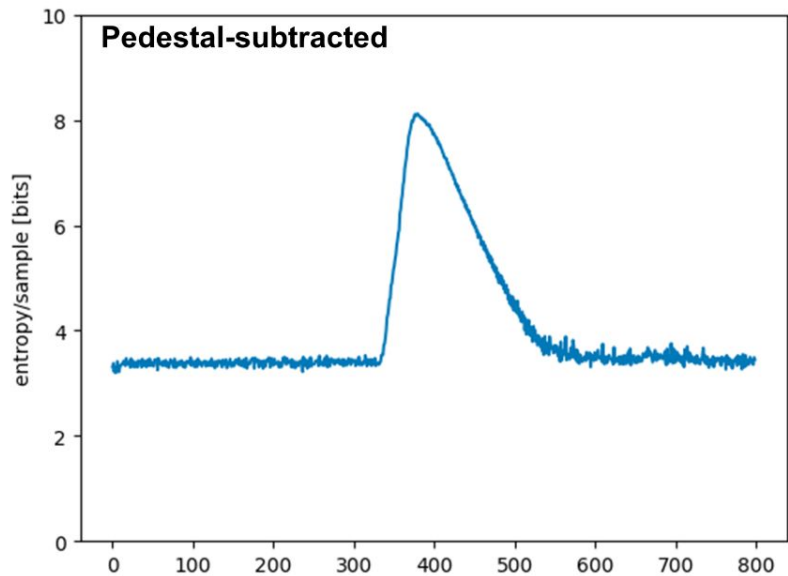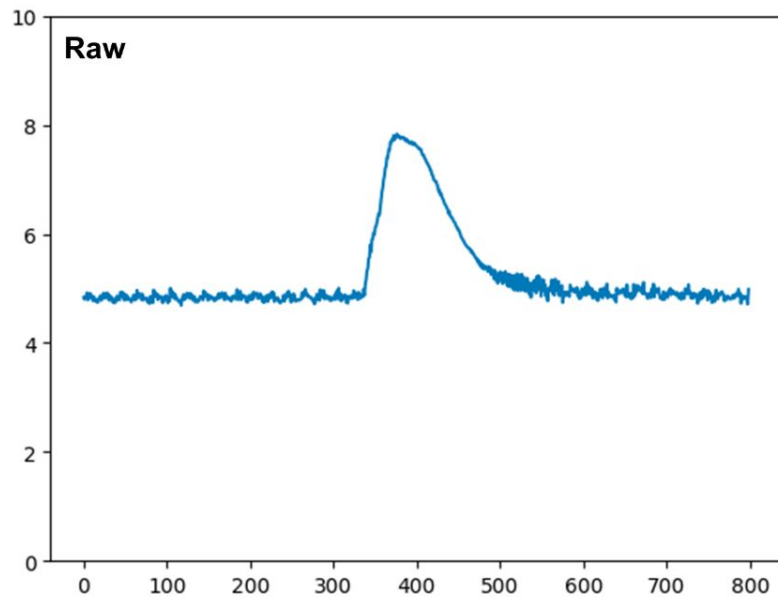
- Entropy reduced for samples near waveform edge: ~3.4 bits

- Average entropy per sample now: 4.05 bits/sample

j.carlton@uky.edu

Discrete Gaussian entropy
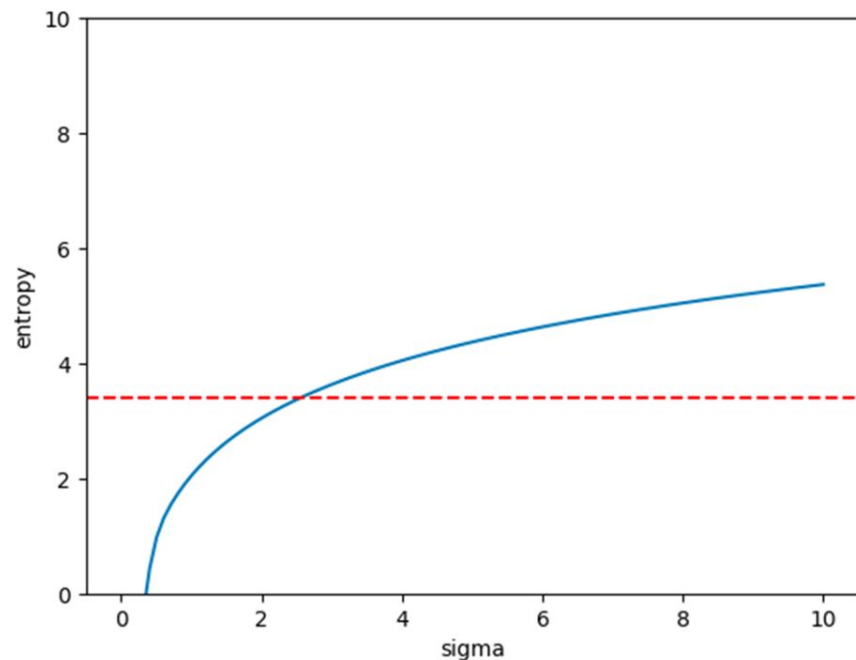
Distribution of ADC values for samples < 200
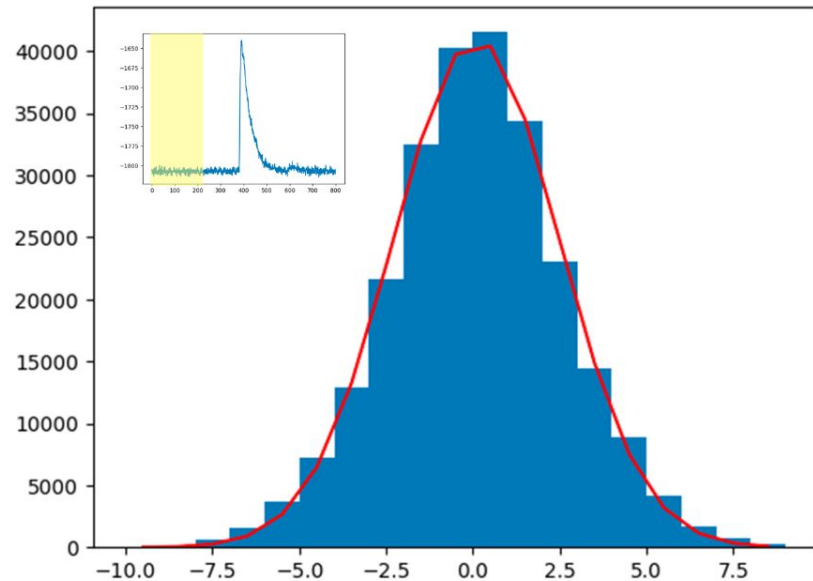
- If we assume gaussian noise: entropy of 3.4 bits -> $\sigma = 2.6$

- If we look at samples < samples number 200 and fit ADC to gaussian: $\sigma = 2.4$

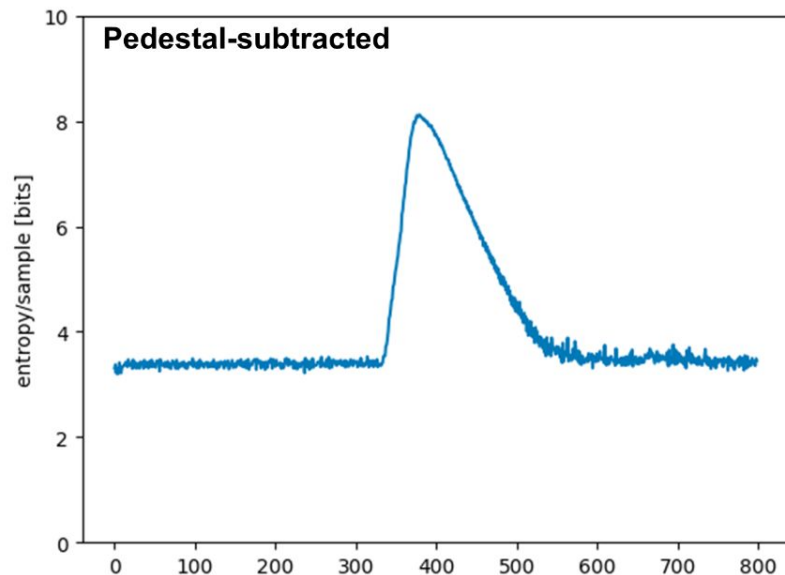# Template fit

- Constructing a template

  - Normalized all traces

  - Time-align the peak

  - Smooth over adjacent sample

  - Fit with $f(t) = A \cdot T(t - t_0) + C$

Example fit

Smoothed

Raw

Normalized

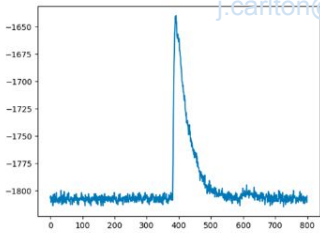Time-aligned

Template fit

j.carlton@uky.edu
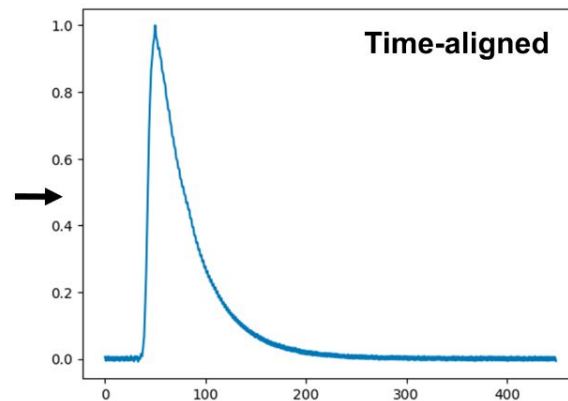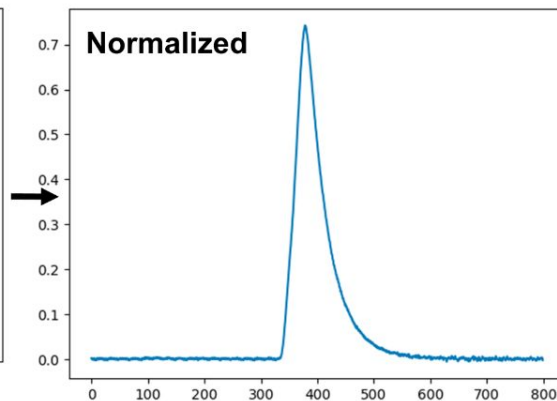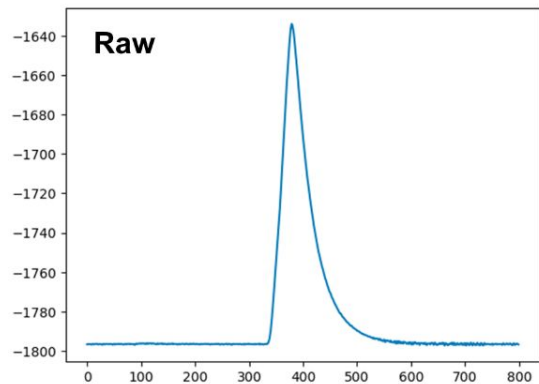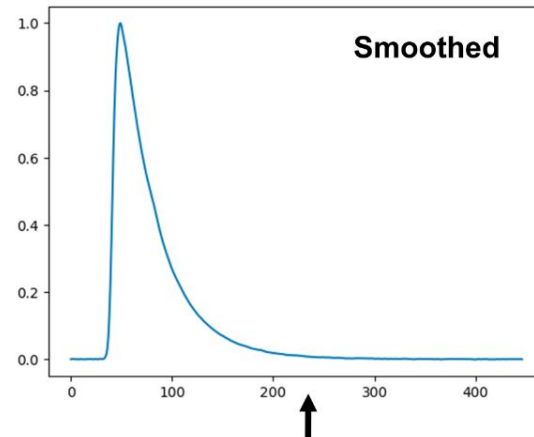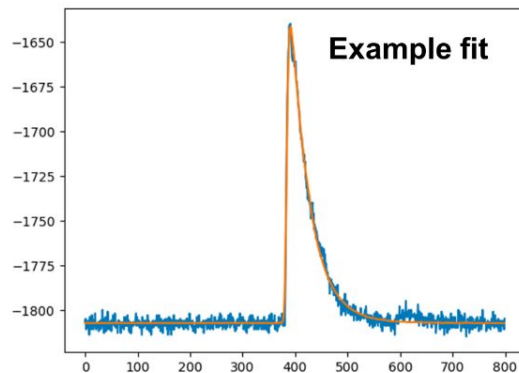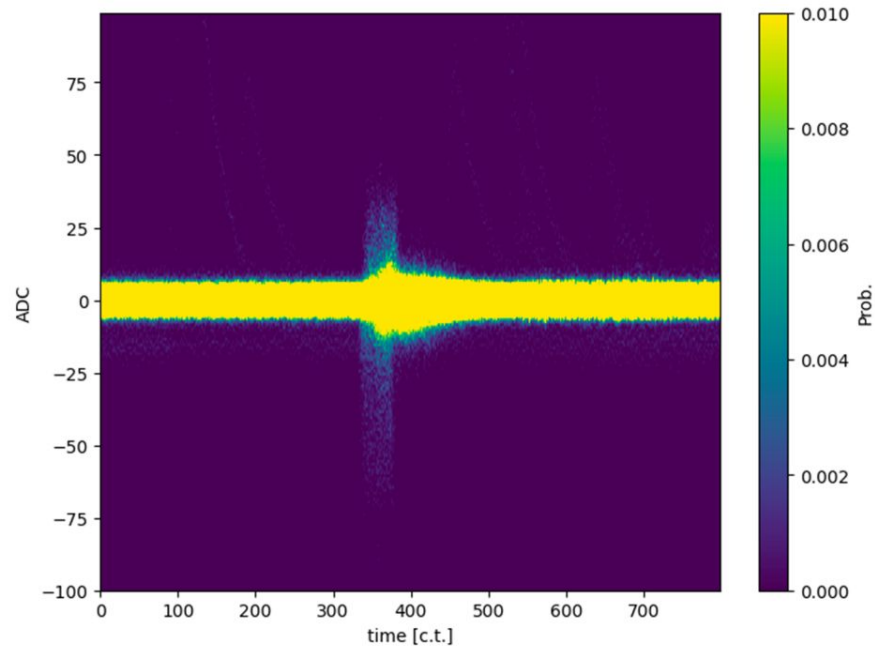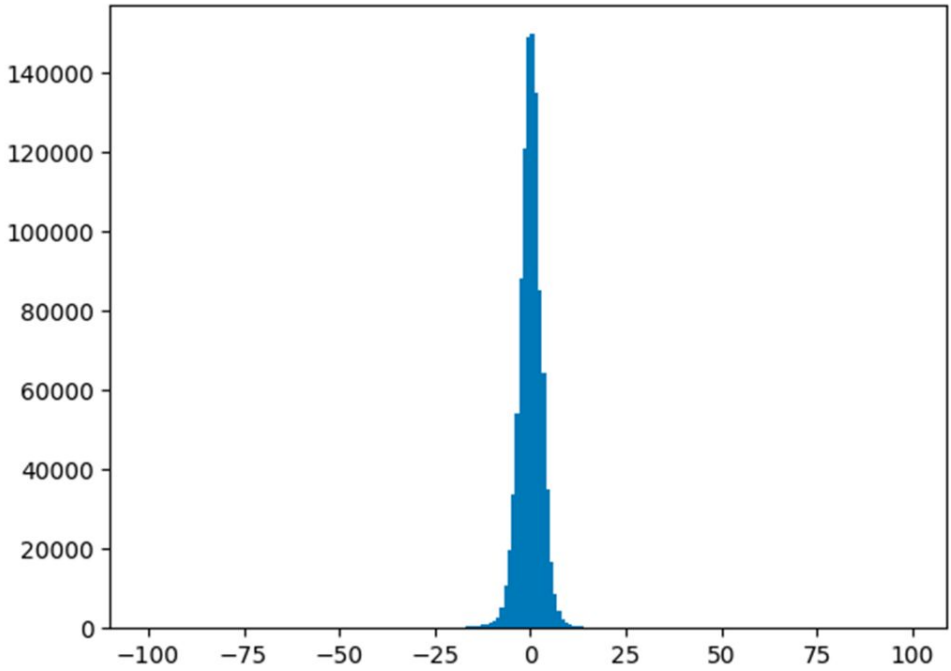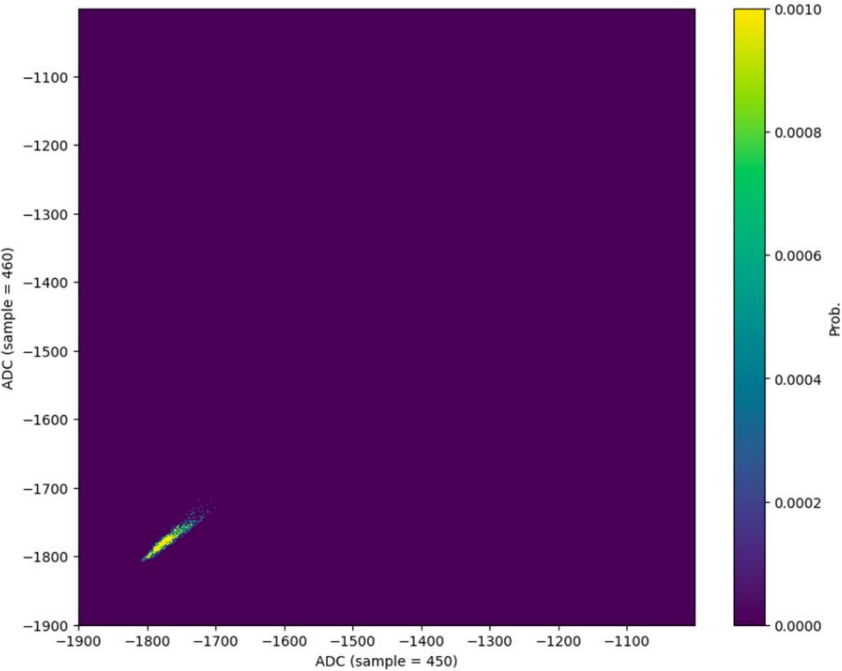
Entropy estimation
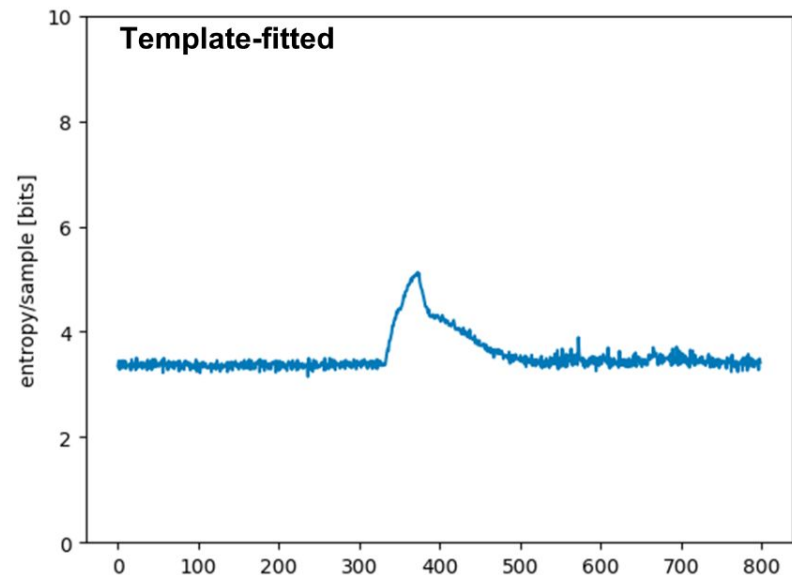
- Baseline hasn't changed much. Makes sense since fluctuations remain

- Peak in middle is reduced, but evidently we can still do better

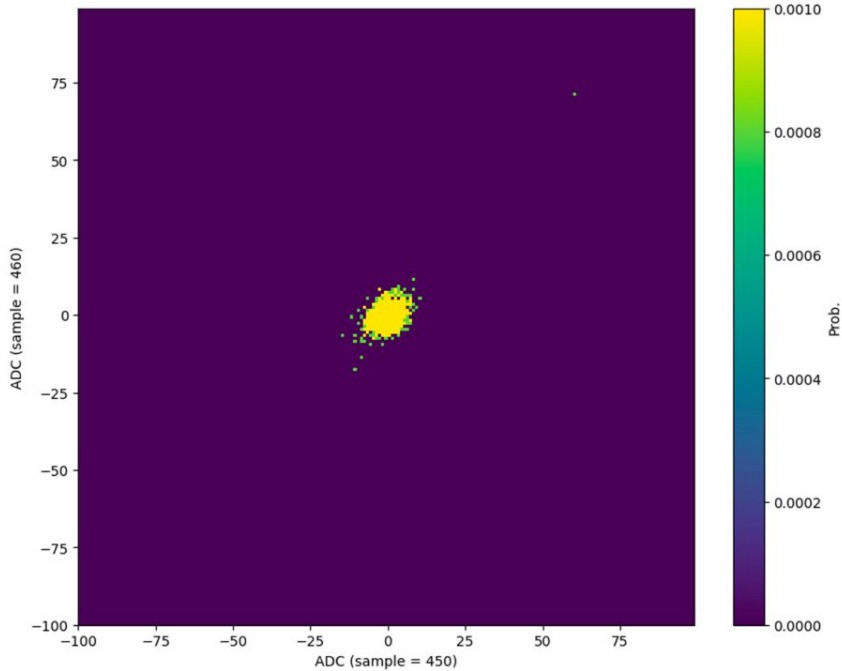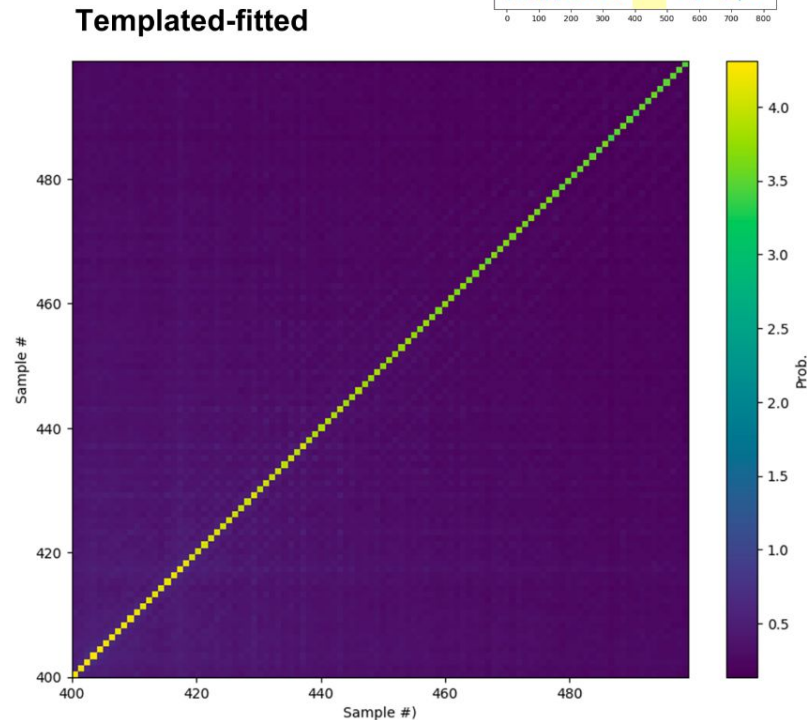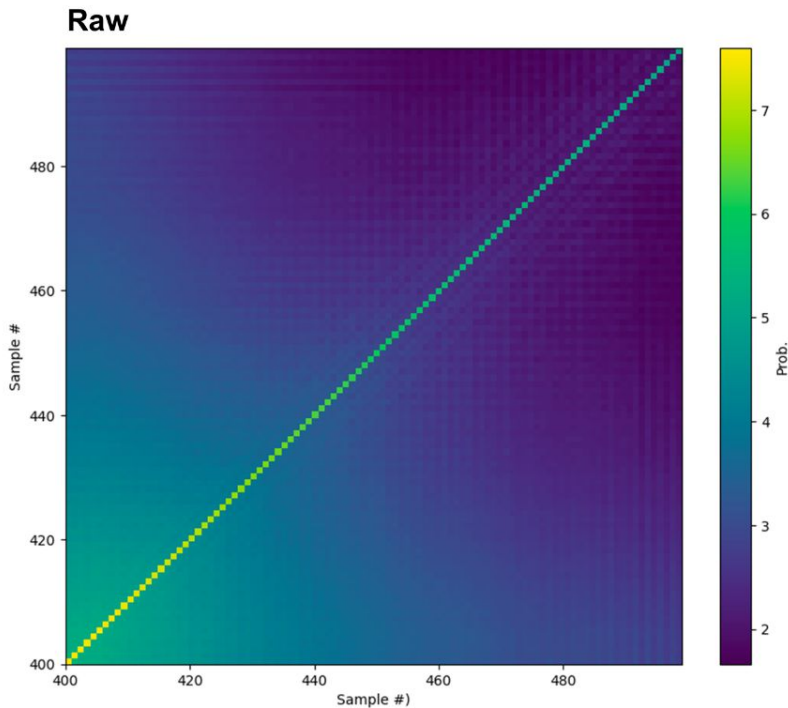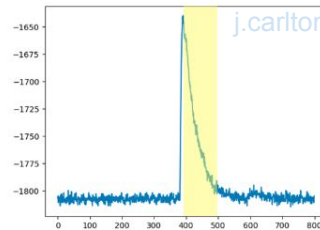- Average entropy per sample now: **3.55 bits/sample**

j.carlton@uky.edu

Correlations

j.carlton@uky.edu

Mutual Information

Raw

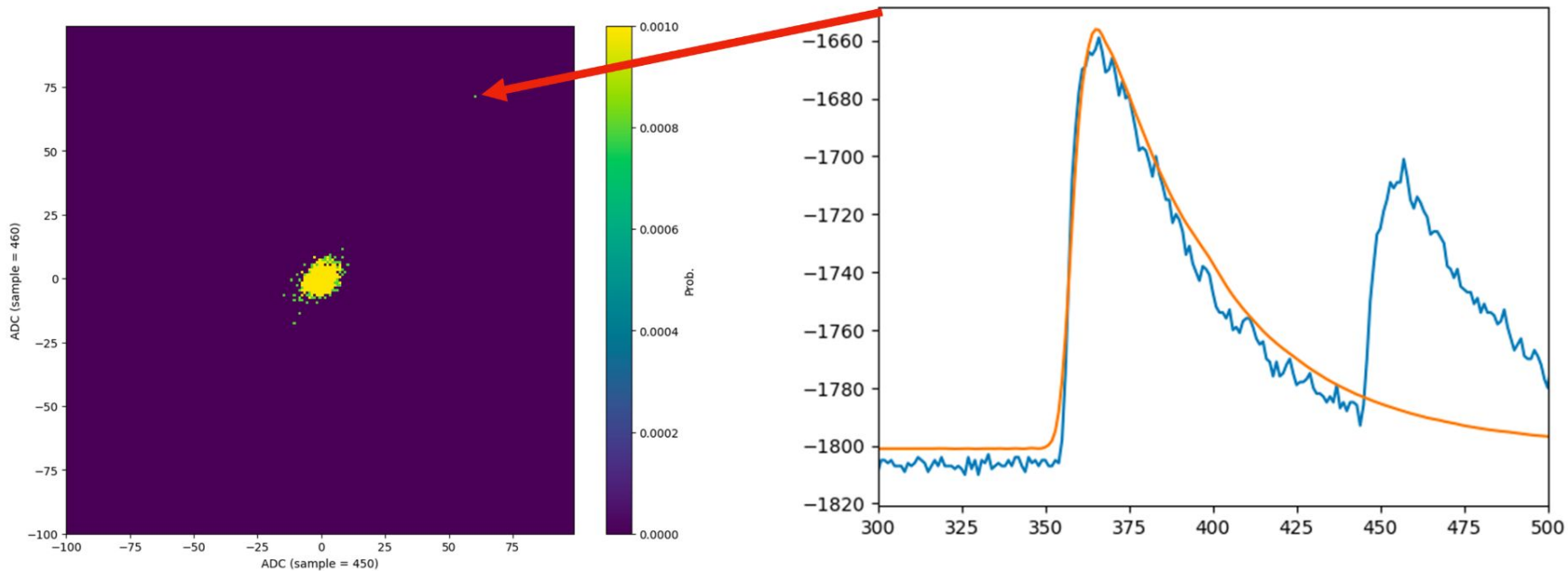**Templated-fitted**

$$H(X) + H(Y) - H(X, Y)$$ **nonzero means there are still correlations**

j.carlton@uky.edu

Template fitting going wrong

- What's causing the spread at the start of the pulse ~360 c.t. or so? (right plot)

- Seems like my template fit going wrong at the pulse turn-on
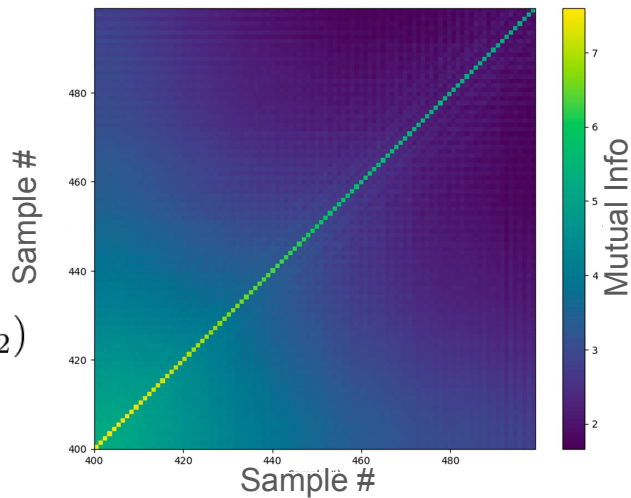
j.carlton@uky.edu
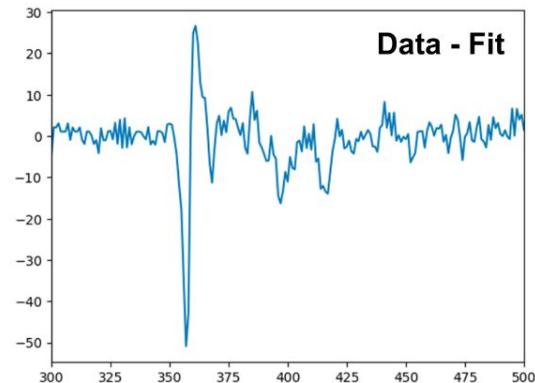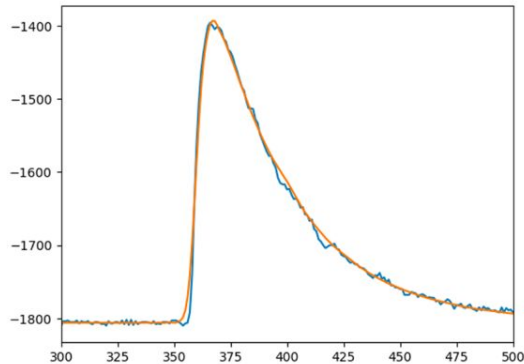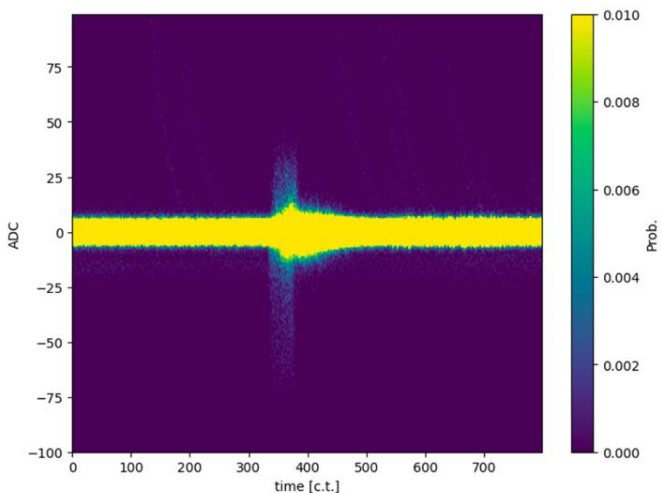
Stray point due to pileup

j.carlton@uky.edu

Mutual Information

- Mutual Information:
  $$I(X_1, X_2) = H(X_1) + H(X_2) - H(X_1, X_2)$$
- $I(X_1, X_2) = 0 \implies$ no correlation
- Template fitting reduces correlations between subsequent samples

Template fitting

j.carlton@uky.edu
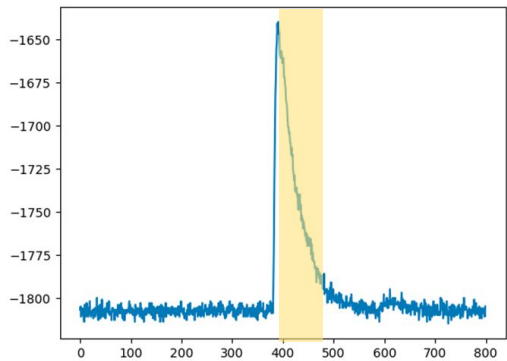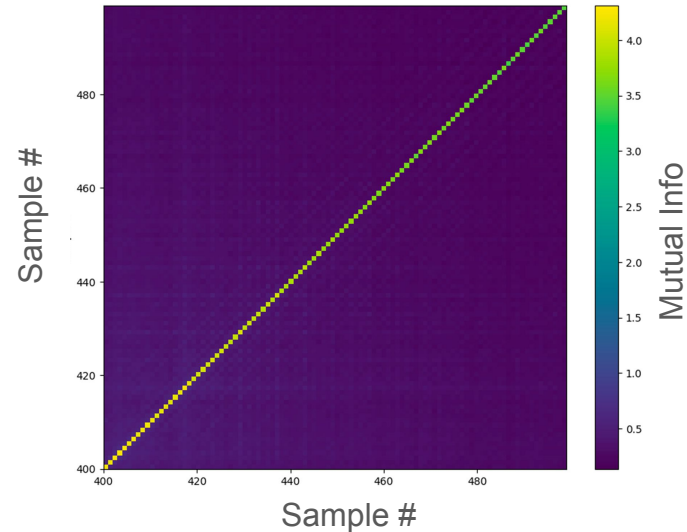
Entropy Estimation

- Average entropy:
$$H_{\mathrm{avg}} = \frac{\sum_{i=1}^{N} H(X_i)}{N}$$

- In this case N = 800

- Before: H_{avg} = 5.22 bits/sample

- After: **H_{avg} = 3.55 bits/sample**

- Some room for improvement(?)
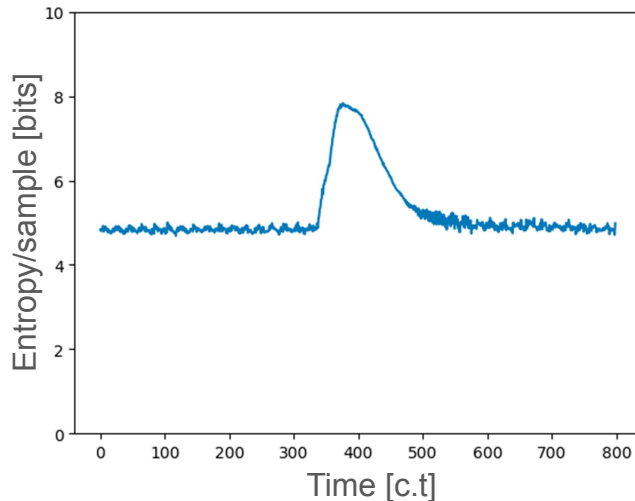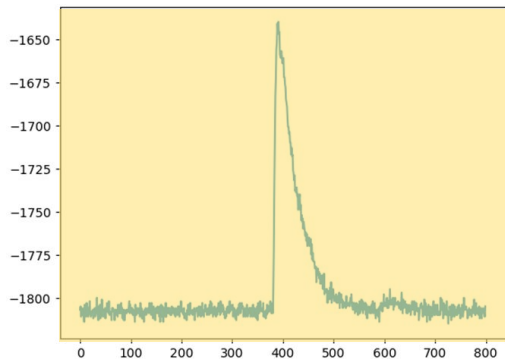
Template fitting
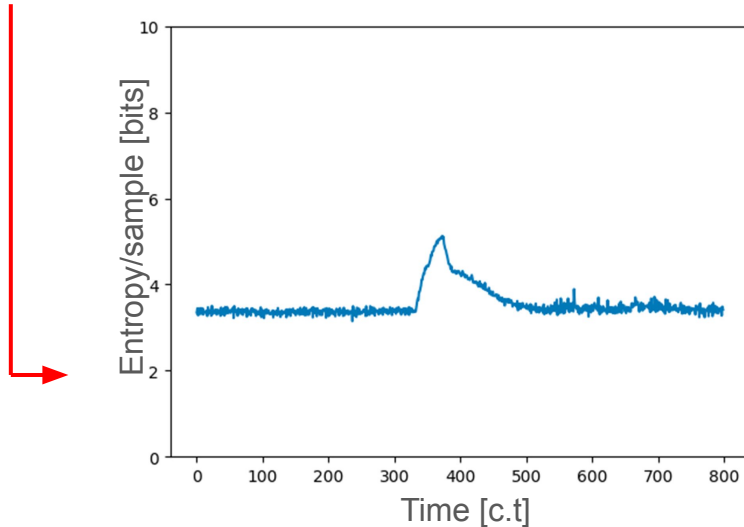
Explanation of Entropy Plot

- The pedestal is easy to fit, so the variance of the pedestal part of the signal is is just the noise of the WFD5s.
  - This is the minimum possible entropy when using this equipment
- The signal is harder to fit and therefore has more variance
  - Entropy of this part of the trace is therefore larger

Entropy Rate of PSI Test Beam Data After Fitting
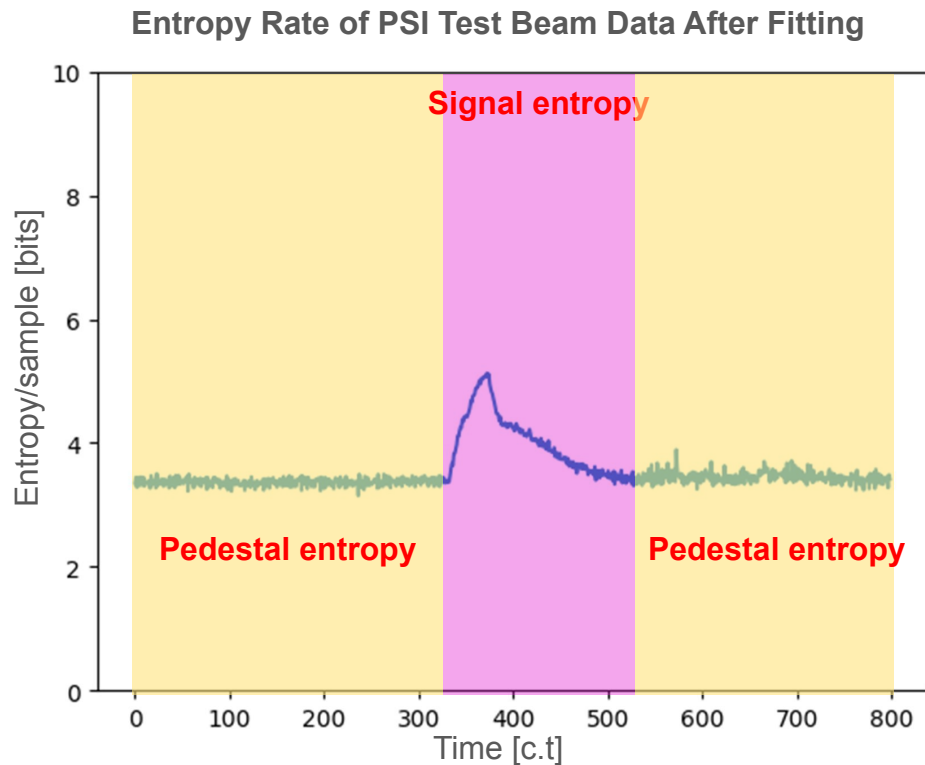
Theoretical Best Compression Calculation

Assuming data is sent as 12 bit ADC samples over PCIe at a data rate of 3.5 GB/s:

$$\text{Compression Ratio} = \frac{\text{Entropy Rate}}{12}$$

$$\text{Storage Data Rate} = \text{Compression Ratio} \cdot 3.5 \text{ GB/s}$$

Entropy rate = 3.4 → New Data Rate ≈ 0.99 GB/s

Entropy rate = 5 → New Data Rate ≈ 1.46 GB/s

Continuing Support for Test Stand DAQ

- Institutions that currently use or plan to use the test stand DAQ in some capacity:
    - CENPA at University of Washington
    - TRIUMF, Canada
    - PSI, Switzerland

- Maintaining and developing software to fit specific needs of each institution

Signal Conditioning

- Want a narrow distribution for compression. Let r_i be the numbers we compress
- Methods tried:
  - No conditioning
  - Delta encoding:
    $r_i = y_{i+1} - y_i$
  - Twice Delta Encoding:
    $r_i = y_{i+2} - 2y_{i+1} + y_i$
  - Double Exponential Fit:
    $r_i = y_i - (A \cdot \exp(at_i) + B \cdot \exp(bt_i))$
  - **Shape Fit**:
    $r_i = y_i - (A \cdot T(t_i - t_0) + B)$

No Conditioning

Signal distribution

Voltage [Arbitrary Units]

Shape Fit

Residuals distribution

Voltage [Arbitrary Units]
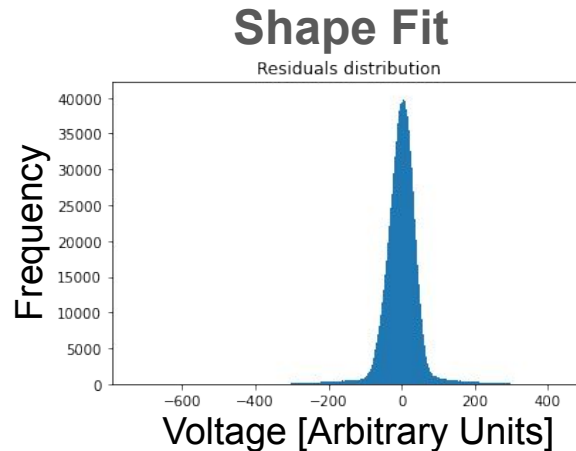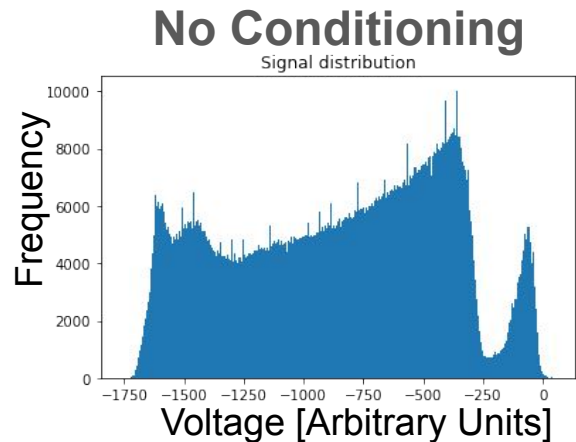
Shape Fitting Algorithm

1. Construct a discrete template from sample pulses
2. Interpolate template to form a continuous Template, *T(t)*
3. "Stretch" and "shift" template to match signal:

$$X[i] = a(t_0)T(t[i] - t_0) + b(t_0)$$

[Note: a and b can be calculated explicitly given t_0]

4. Compute χ^2 (assuming equal uncertainty on each channel i)

$$\chi^2 \propto \sum_i \{X[i] - a(t_0)T(t[i] - t_0) + b(t_0)\}^2$$

5. Use Euler's method to minimize χ^2

Lossless Compression Algorithm

- Rice-Golomb Encoding
  - Let x be number to encode

    y = "s"+"q"+"r"
    - q = x/M (unary)
    - r = x%M (binary)
    - s = sign(x)
  - Any distribution
  - Close to optimal for valid choice of M
  - One extra bit to encode negative sign
  - Self-delimiting
  - If quotient too large, we "give up" and write x in binary with a "give up" signal in front
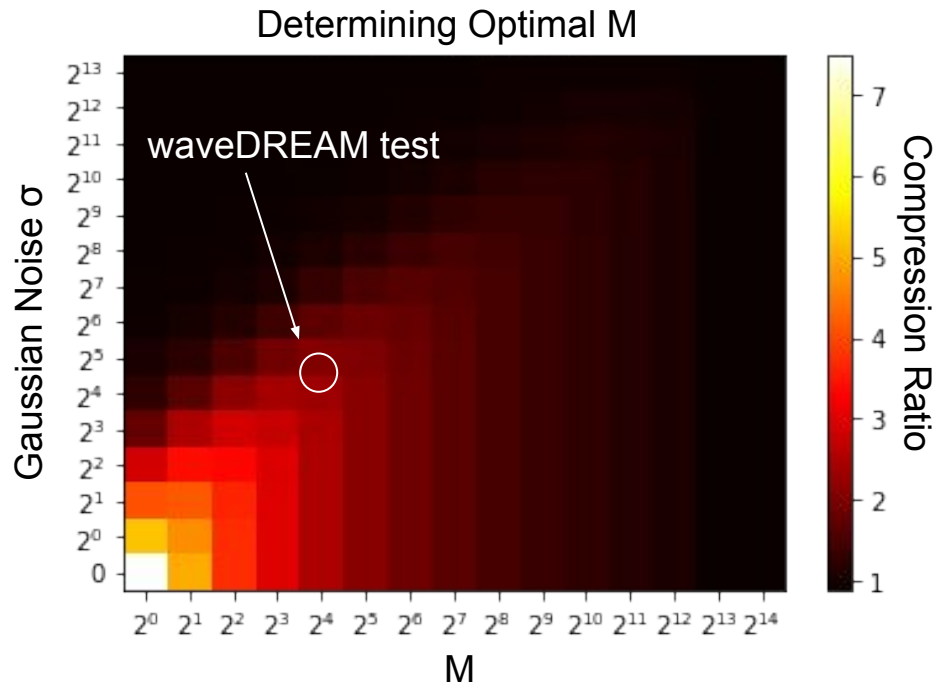
Rice-Golomb Encoding (M=2)

Value	Encoding
-1	011
0	000
1	001
2	1000

Red = sign bit
Blue = quotient bit(s) (Unary)
Yellow = remainder bit (binary)

How to choose Rice-Golomb parameter M

- Generated fake Gaussian data (centered at zero) with variance σ^2

- For random variable X, $M \approx \text{median}(|X|)/2$ is a good choice
  - This is the close to the diagonal on the plot

- $\sigma \approx 32$ for residuals of shape on wavedream data $\to$ M = 16 is a good choice
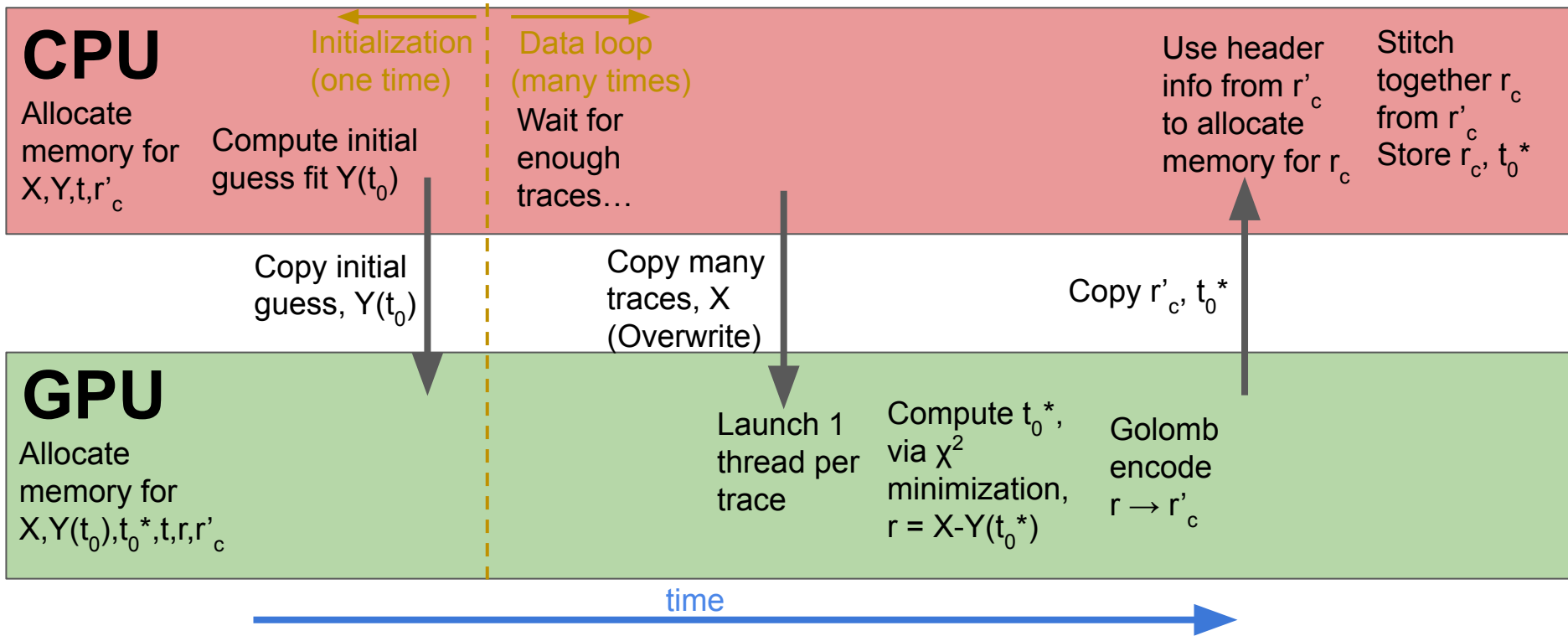

Determining Optimal M

waveDREAM test

Compression Ratio from Rice-Golomb Encoding

- Lossless compression factor of ~2

- In agreement with plot from simulated data on last slide

- Best compression ratio we achieved

Rice-Golomb Compression on Residuals (M = 16)

Compression Ratio

Sample Index
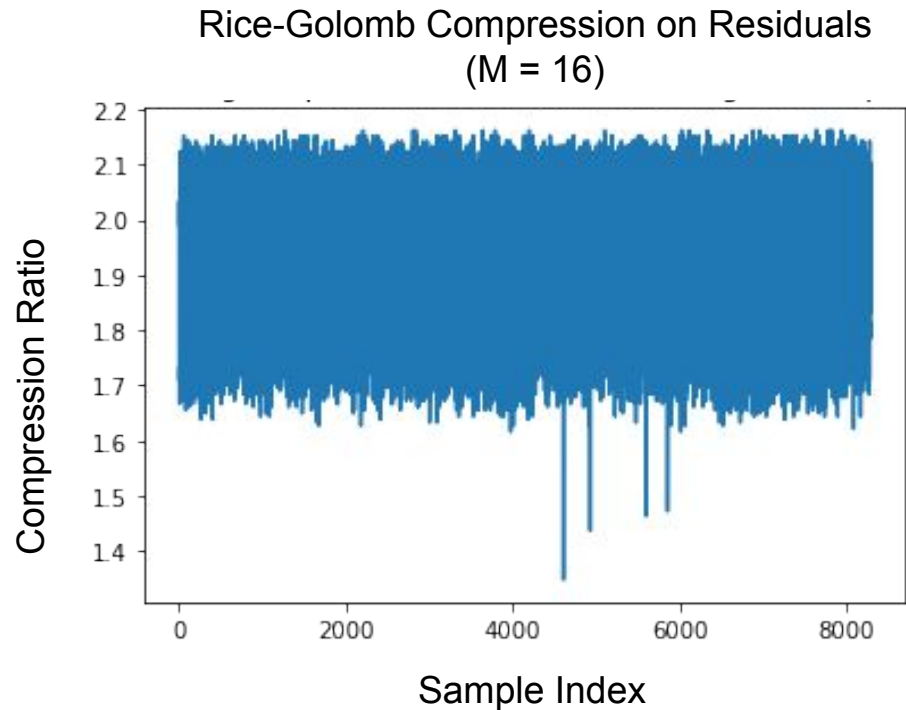
Real Time Compression Algorithm

- We choose to let the FE's GPU and CPU handle compression for flexibility

CPU

Initialization (one time) | Data loop (many times)

Allocate memory for X, Y, t, r'_c

Compute initial guess fit $Y(t_0)$

Wait for enough traces...

Use header info from r'_c to allocate memory for r_c

Stitch together r_c from r'_c Store r_c, t_0^*

Copy initial guess, $Y(t_0)$

Copy many traces, X (Overwrite)

Copy r'_c, t_0^*

GPU

Allocate memory for $X, Y(t_0), t_0^*, t, r, r'_c$

Launch 1 thread per trace

Compute t_0^*, via χ^2 minimization, $r = X - Y(t_0^*)$

Golomb encode $r \rightarrow r'_c$

time

GPU Benchmarking (Timings)

- ● Block Size:
  - ○ A GPU parameter, number of threads per multiprocessor

- ● Can compress 2^{26} integers (32-bit) in roughly ⅓ of a second.
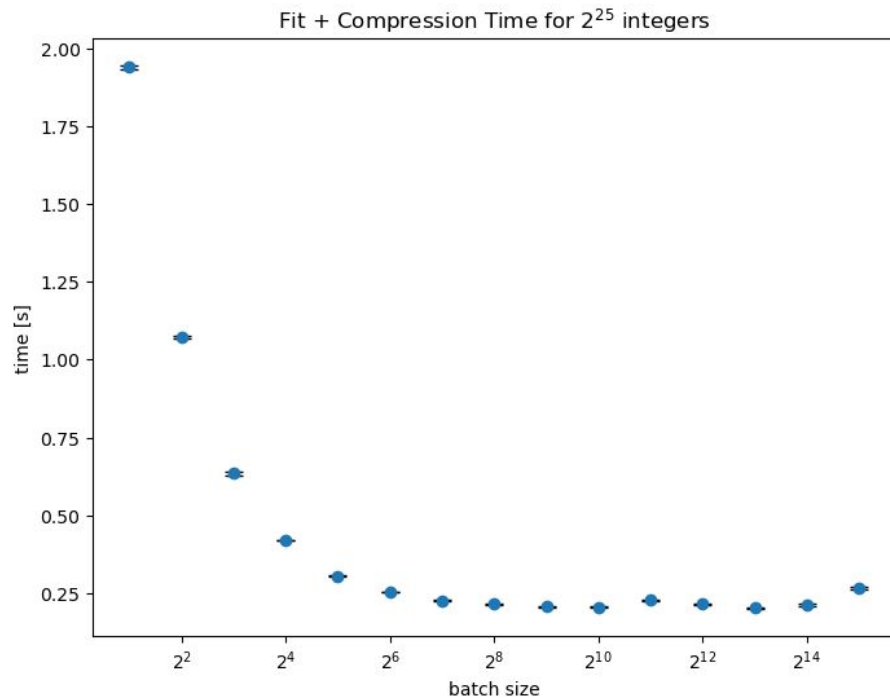 - → ~ **0.8 GB/s** compression rate

Fit + Compression Time using A5000 in PCIe4
(Batch Size = 1024)
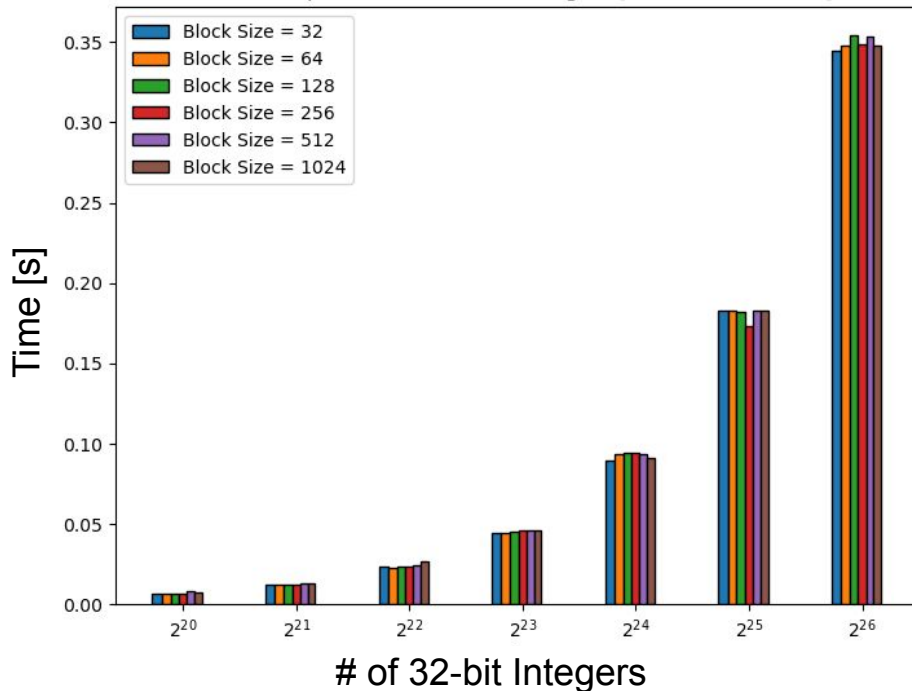
GPU Benchmarking (Timings)

- Batch Size:
  - How many integers are compressed by a single GPU thread

- Data must be sent to GPU in batches (not a continuous flow) to take full advantage of parallel computation

Fit + Compression Time for 2^{25} integers

FPGA Firmware Design

FPGA Firmware Ideas

- Vivado allows [creating custom AXI IP blocks](#)
- This could allow for periodically editing registers in the on board RAM by using a AXI IP block to communicate between FPGA and RAM
  - Allows for simulating data acquisition and reading in data based on "control" registers
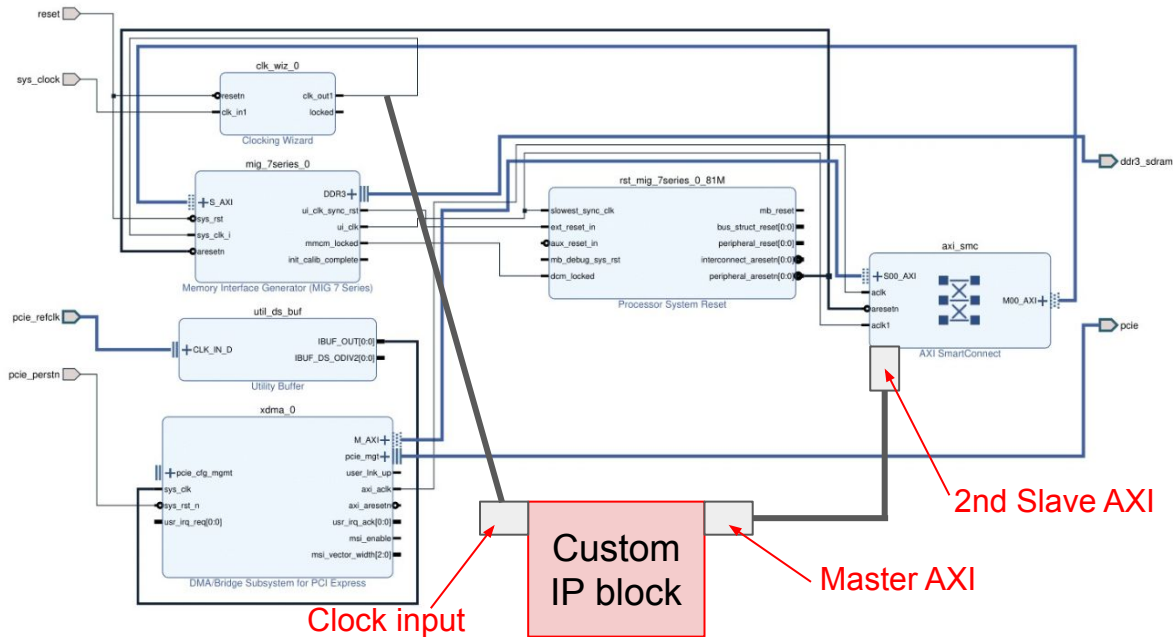
Block diagram for PCIe DMA transfer with proposed custom IP block connection